Thèse présentée pour obtenir le grade de
Docteur de l'Université Louis Pasteur
Strasbourg I

Discipline : Sciences Odontologiques

par Héctor FLORES

Auto-assemblage de polyélectrolytes : formation de nanoring, adhésion de protéines et de cellules

Soutenue publiquement le 05 Juillet 2005

Membres du jury :

Directeur de Thèse :	**M. Frédéric CUISINIER**	**Docteur**	**Université Louis Pasteur**
Co-directeur de Thèse :	**M. Elias PEREZ**	**Professeur**	**University of San Luis Potosí**
Rapporteur Interne :	**M. Jacques HAIECH**	**Professeur**	**Université Louis Pasteur**
Rapporteur Externe:	**M. Henry MAGLOIRE**	**Professeur**	**Université de Lyon I**
Rapporteur Externe:	**M. Ricardo ESPINOSA**	**Professeur**	**University Western Ontario**
Examinateur :	**Mme. Csilla GERGELY**	**Professeur**	**Université Montpellier II**

Thesis presented by
Hector FLORES

To obtain the title of Doctor of the
Université Louis Pasteur
Strasbourg I
Specialty: Odontologic Sciences

Self-Assembly Polyelectrolytes: nanoring formation, protein and cell adhesion

05 July 2005

Table of Contents

Chapter I **10**
1 Physical and Chemical Properties of Polyelectrolytes **10**
1.1 Basic Concepts in Polyelectrolytes **11**
1.2 Natural and artificial polyelectrolytes **12**
1.2.1 Natural polyelectrolytes *12*
1.2.1.1 The polysaccharides *12*
1.2.1.2 Polypeptides *13*
1.2.1.3 Acid/basic properties *15*
1.2.1.4 Proteins *16*
1.2.1.5 The polynucleotide: DNA *18*
1.2.2 Synthetic polymers (artificial polyelectrolytes) *19*
1.3 Polyelectrolyte charge classification **20**
1.3.1 Weak and Strong polyelectrolytes *21*
1.3.1.1 Weak polyelectrolytes *21*
1.3.1.2 Strong polyelectrolytes *22*
1.4 Ion dissociation into a solvent **22**
1.4.1 Quality of the solvents *23*
1.4.2 Polyelectrolyte water behavior classification *23*
1.5 Polyelectrolyte effects **23**
1.6 General behavior of polyelectrolytes in solution **24**
1.6.1.1 Structure of hydrophobic polyelectrolytes in poor solvents *25*
1.6.1.2 Necklace Globule *26*
1.6.1.3 Monte Carlo simulation *26*
1.6.1.4 Ionic strength effect on polyelectrolytes conformation in solution *28*
1.6.1.5 Polyelectrolyte domains formation in solution *30*
1.7 Adsorption of hydrophobic polyelectrolytes at oppositely charged surfaces **31**
1.7.1 Substrates *33*
1.7.1.1 Polyelectrolyte-substrate interaction *34*
1.8 Conclusion **35**
1.9 Bibliography **37**
Chapter II **38**
2 Materials and Methods **38**
2.1 Introduction **39**
2.2 AFM Microscope **39**
2.2.1 Piezoelectric ceramic transducer *40*
2.2.2 Operate modes *41*
2.2.3 Principle *42*

2.2.3.1 Tip-sample interaction mode *42*
2.2.4 Experimental method *43*
2.3 Micro-peeling aspiration technique **44**
2.3.1 Quantification of Cell Adhesion *44*
2.3.2 Experimental method *46*
2.4 Transmission electron microscope **48**
2.4.1 Experimental methods *48*
2.5 Ultra violet spectroscopy **48**
2.5.1.1 Fluorescence *49*
2.5.1.2 Intra-molecular redistribution of energy between possible electronic and vibrational states *49*
2.5.1.3 Chemiluminescence *50*
2.5.2 Experimental method *50*
2.6 Materials **50**
2.6.1 Polyelectrolytes *50*
2.6.2 Polyelectrolyte nanorings formation method *51*
2.6.3 Nanoparticles synthesis *52*
2.6.3.1 Experimental method *52*
2.7 Bibilography **53**
Chapter III **54**
3 SAPF Functionalization: Protein Adsorption and Cell Adhesion **54**
3.1 Introduction **55**
3.2 Self Adsorption of Polyelectrolyte Films (SAPF) **55**
3.3 SAPF Protein Functionalization **57**
3.4 Article 1 ..... **58**
3.5 SAPF Protein Functionalized and Cell Adhesion Test **66**
3.6 Article 2 ..... **68**
3.7 Bibliography **69**
Chapter IV **70**
4 Polyelectrolyte Nanoring Structures **70**
4.1.1 Introduction *71*
4.1.2 Article 3 ..... *73*
4.1.3 Article 4 ..... *82*
Chapter V **88**
5 Polyelectrolyte structures as Pattern for Quantum Dots Assembly **88**
5.1 Introduction **89**
5.2 Polyelectrolyte Nanoring Structures as Nano-patterning for Polyelectrolyte Quantum Dot Assembly **89**
5.2.1 Experimental section: *90*
5.3 Results and discussion **90**
5.4 Conclusions **95**

5.5 Bibliography 96
6 Conclusions and Perspectives 97

Introduction

Materials interact with their environments through surfaces and interfaces. Therefore many strategies have been developed for the chemical modification of surfaces. In the past decade the field on nanostructured materials design has progressed significantly. A greater understanding of the manipulation of matter at nanoscale level has lead to a number of advances in materials science, ranging from the development of novel optical and electronic properties to the formation of high strength materials which imitate nature to stimuli responsive materials applicable to a range of applications.

The key role of surfaces for many material properties as well for many biological processes has been recognized now. Several methods of nanostructures materials have been developed in the past few decades; among these techniques are chemical vapour deposition, atomic layer deposition, colloid assembly and molecular bean epitax.

Many of these approaches require a fairly well controlled environment and sophisticated equipment, and therefore, involve high capital and operating costs. New strategies aim to tailor materials surface only, while preserving the bulk properties of the underlying support. Particular emphasis has been given to surface modification by polymers, in an attempt to extend the known versatility of polymer bulk materials to form ultrathin films and coatings, and to prepare bulk-surface composite materials.

The self-organization of polymers has been increasingly explored for the preparation of well-defined surfaces and interfaces in recent years extending the use of the established methods of low molar mass compounds. With such techniques, polymer films are formed spontaneously on substrates, due to balanced interactions between substrate, polymer and medium. Typically, very thin, often monomolecular layers are produced. Repetitive deposition steps allow a precise control over the total thickness of the coatings, in range from a few angstroms up to the micrometer range. Moreover, the step-by-step procedures allow a fine structuring in the third dimension.

The most recent of self-organization techniques is the alternating physisorption of oppositely charged polyelectrolytes, so-called layer-by-layer (L-b-L) method or electrostatic self-assembly (ESA). A decade ago Decher demonstrated the basic principle, the alternating exposure of a charged substrate to solutions of positive or negative polyelectrolytes, respectively provide that each

adsorption step leads to charge inversion of the surface, the subsequent deposition finally result in a layered complex, stabilised by strong electrostatic forces. The versatility of the multilayer formation process with respect to the variety of materials which can be used as building blocks, and furthermore the possibility of combination with other assembly procedures result a high application potential in a broad range of different areas of materials development. This method can be used to create highly tuned, functional thin films at nanometer level control of film composition and structure.

One of the most significant characteristic of the polyelectrolytes is the possibility of intercalating and of immobilizing a large variety of made up on treated surface, such as inorganic particles or organics as proteins, enzymes, etc, providing to the material really active characteristics, constitute by new strategies to design biomaterials which manage the answer of the host.

Our work focused on the following aspects:

- The study of proteins adsorption on films with a particular pH
- The study by micro aspiration of cells adhesion onto polyelectrolytes films
- The study of the formation of polyelectrolytes nanoring

We studied the adsorption of the HSA on films made of polypeptides, the poly(L-lysine) (PLL), and the acid poly(glutamique) (PGA) in different pH ranged from 3.0 to 10.5.

We studied also the adhesion of cells on polyelectrolytes films. All the biological processes are achieved thanks to weak specific molecular interactions which generate connections of short time. Strong interactions would remove all dynamics essential to the life. Then, we evaluated by a micropipette micromanipulation technique the short-term interactions of cells with multilayer films. The goal of this work was the modulation of the multilayer film properties with respect to the cellular adhesion.

Finally, we observed at the time of deposit of PSS on a layer of PEI, the formation of spherical structures. We call these structures nanorings due to their shape and size-thickness rate. The structure sizes ranged from 300 nm to 2 µm diameter among different experiments but by experiment, they are very homogeneous. Such structures had never been observed. Then, our work was aimed also to understand the mechanisms that govern the formation of these structures. The experiments were realized in an AFM microscope by using a liquid-cell technique which prevents the form of artefacts due to dehydration.

Chapter I

1 Physical and Chemical Properties of Polyelectrolytes

Chapter I **10**
1 Physical and Chemical Properties of Polyelectrolytes **10**
1.1 Basic Concepts in Polyelectrolytes **11**
1.2 Natural and artificial polyelectrolytes **12**
1.2.1 Natural polyelectrolytes *12*
1.2.1.1 The polysaccharides *12*
1.2.1.2 Polypeptides *13*
1.2.1.3 Acid/basic properties *15*
1.2.1.4 Proteins *16*
1.2.1.5 The polynucleotide: DNA *18*
1.2.2 Synthetic polymers (artificial polyelectrolytes) *19*
1.3 Polyelectrolyte charge classification **20**
1.3.1 Weak and Strong polyelectrolytes *21*
1.3.1.1 Weak polyelectrolytes *21*
1.3.1.2 Strong polyelectrolytes *22*
1.4 Ion dissociation into a solvent **22**
1.4.1 Quality of the solvents *23*
1.4.2 Polyelectrolyte water behavior classification *23*
1.5 Polyelectrolyte effects **23**
1.6 General behavior of polyelectrolytes in solution **24**
1.6.1.1 Structure of hydrophobic polyelectrolytes in poor solvents *25*
1.6.1.2 Necklace Globule *26*
1.6.1.3 Monte Carlo simulation *26*
1.6.1.4 Ionic strength effect on polyelectrolytes conformation in solution *28*
1.6.1.5 Polyelectrolyte domains formation in solution *30*
1.7 Adsorption of hydrophobic polyelectrolytes at oppositely charged surfaces **31**
1.7.1 Substrates *33*
1.7.1.1 Polyelectrolyte-substrate interaction *34*
1.8 Conclusion **35**
1.9 Bibliography **37**

1.1 Basic Concepts in Polyelectrolytes

A polyelectrolyte, by definition, is a chemical compound that upon being placed in water or any other ionizing solvent dissociates into a charged polymeric molecule. In other words, small ions dissociate from the macromolecule, leaving a net charge associated with the chain. This unique chemical property allows a great variety of applications.

Practical applications of polyelectrolytes hinge upon the fact that these materials are: (a) water soluble polymers capable of promoting major changes in the fluid properties of aqueous suspensions and slurries; (b) substances which may be absorbed by neutral particles, thus imparting a surface charge; (c) substances whose ionized groups interact very strongly with ions and colloidal aggregates of opposite charge; and (d) substances which can be tailored to be sensitive or insensitive to chemical and biological degradation. Polyelectrolytes find applications as thickeners, dispersants, water conditioners, waste treatment agents, soap and detergent additives, soil conditioners, ion-exchange resins, and enhanced oil recovery agents.

In addition to their essential function in human physiology and cellular mechanism in the formation of proteins, polypeptides and nucleic acids, polyelectrolytes have found a number of important applications in the major fields of science and engineering such as chemistry, physics, chemical and materials engineering. However, polyelectrolytes belong to the least understood materials in the condensed matter area, despite the fact that they are everywhere around and in us.

In this chapter a general overview of polyelectrolytes origin will be given as well as a brief review of the physical and chemical properties of polyelectrolytes that makes them of interest for industry and medicine.

1.2 Natural and artificial polyelectrolytes

Polymers with bound positive or negative charges are referred to polyelectrolytes, macroions, or polyions. These polymers may be synthetic or natural.

1.2.1 Natural polyelectrolytes

There are many molecules that are important for life on Earth. Most molecular constituents of living systems are composed of carbon atoms covalently joined with other carbon, hydrogen, oxygen or nitrogen atoms. The special bonding properties of carbon permit the formation of a great variety of molecules such as amino acids (protein constituents), nucleotides (DNA) constituents and monosaccharide (glucose units).

1.2.1.1 The polysaccharides

Polysaccharides have been proposed as the first biopolymers to have formed on Earth. They are classified on the basis of their main monosaccharide components and the sequences and linkages between them, as well as the anomeric configuration of linkages, the ring size (furanose or pyranose), the absolute configuration (D- or L-) and any other constituents present. There are neutral polysaccharides as amidon, cellulose (constituent of the cell walls in plant cells) and glycogen (storage of glucose in animals).

The other polysaccharides are charged, and represent the largest part of natural polyelectrolytes. One of the most important polysaccharides are the alginates. Alginates are linear unbranched polymers containing β-(1→4)-linked D-mannuronic acid (M) and α-(1→4)-linked L-guluronic acid (G) residues (Fig.1). Alginates are produced by brown seaweeds (Phaeophyceae, mainly Laminaria). Alginate is gelling at far lower concentrations than gelatine. Such gels can be heat treated without melting, although they may eventually degrade.

Hyaluronic acid is one of the most hydrophilic (water-loving) molecules in nature and can be described as "nature's moisturizer". The molecule of hyaluronic is made up of a repetitive sequence of two modified simple sugars, one called glucuronic acid and the other N-acetyl glucosamine (Fig.1). These compounds are both negatively charged and when put together; they repel producing an exceptionally long stretched out molecule (high molecular weight). In the body, hyaluronic acid always presents itself as a large high molecular weight molecule.

There are also cationic polyelectrolytes. The chitosan is the most abundant (second compound in the biomass after the cellulose). The molecule of chitosan is made up of a repetitive sequence of beta-(1,4)-2-amino-2-deoxy-D-glucose, or poly-D-glucosamine, or poly N-acetyl-D-glucosamine (Fig.1). Chitosan is derived from chitin, a polysaccharide found in the exoskeleton of shellfish such as shrimp, lobster, and crabs. The charge comes from the amino group. However, the chitosan are not charged at weak pH.

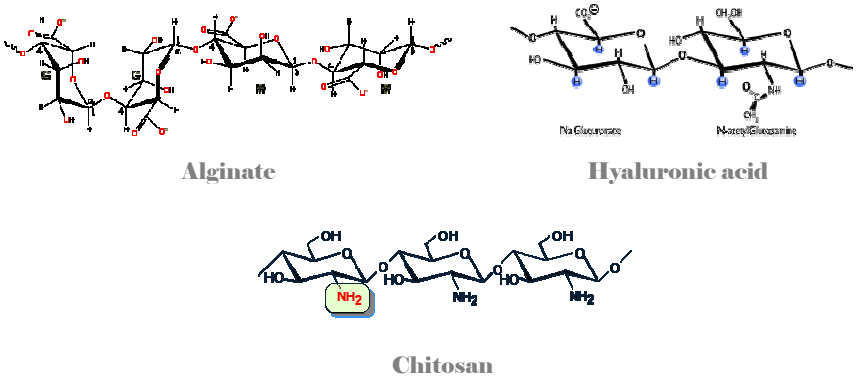

Fig. 1 Chemical structure of three linear polysaccharides that are natural polyelectrolytes. The alginate is mainly used in the alimentary industry. The hyaluronic acid is a cellular activity promoter. For these two polysaccharides, the charge is given by the carboxyl group. The chitosan is a cationic polysaccharide. The charge comes from the amino-group.

1.2.1.2 Polypeptides

Proteins consist of amino acids which are characterized by the -CH(NH_2)COOH substructure (see Fig. 2). Nitrogen and two hydrogens comprise the amino group, -NH_2, and the acid entity is the carboxyl group, -COOH. Amino acids link to each other when the carboxyl group of one molecule reacts with the amino group of another molecule, creating a peptide bond -C(=O)NH- (Fig.2) and releasing a molecule of water (H_2O).

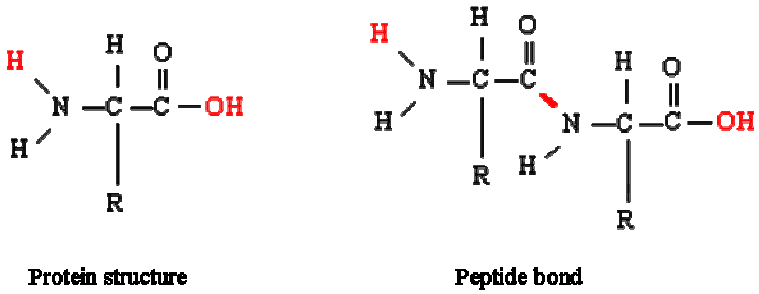

Fig. 2 Basic chemical structure of a protein (left) characterized by the presence of -CH(NH_2)COOH groups and an example of peptide bond (right) indicated in red.

Amino acids are the basic building blocks of enzymes, hormones, proteins, and body tissues. A peptide is a compound consisting of 2 or more amino acids. Oligopeptides have 10 or less amino

acids. Polypeptides and proteins are chains of 10 or more amino acids, but peptides consisting of more than 50 amino acids are classified as proteins.

A list of the 20 essential amino acid is presented in table I

Table I. The 20 natural amino acids.

Name	**Abbrev.**	**Group**	**Chemical Structure**	**Properties**
Alanine	Ala	A	$CH_3CH(NH_2)COOH$	Hydrophobic neutral
Arginine	Arg	R	$H_2N\text{-}C(=NH)NHCH_2CH_2CH(NH_2)COOH$	Hydrophilic cationic at pH><pKa
Asparagine	Asn	N	$H_2N\text{-}C(=O)CH_2CH(NH_2)COOH$	Hydrophilic neutral to moderate
Aspartic acid	Asp	D	$HOOC\text{-}CH_2CH(NH_2)COOH$	Hydrophilic anionic at pH>pKa
Cysteine	Cys	C	$HS\text{-}CH_2CH(NH_2)COOH$	Hydrophilic anionic at pH>pKa
Glutamine	Gln	Q	$H_2N\text{-}C(=O)CH_2CH_2CH(NH_2)COOH$	Hydrophilic neutral to moderate
Glutamic acid	Glu	E	$HOOC\text{-}CH_2CH_2CH(NH_2)COOH$	Hydrophilic anionic at pH>pKa
Glycine	Gly	G	$H_2N\text{-}CH_2COOH$	Amphiphilic neutral
Histidine	His	H	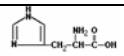	Hydrophilic cationic at pH><pKa
Isoleucine	Ile	I	$CH_3CH_2CH(CH_3)CH(NH_2)COOH$	Hydrophobic neutral
Leucine	Leu	L	$CH_3CH(CH_3)CH_2CH(NH_2)COOH$	Hydrophobic neutral
Lysine	Lys	K	$H_2N\text{-}CH_2CH_2CH_2CH_2CH(NH_2)COOH$	Hydrophilic cationic at pH><pKa
Methionine	Met	M	$CH_3\text{-}S\text{-}CH_2CH_2CH(NH_2)COOH$	Hydrophobic neutral
Phenylalanine	Phe	F	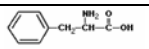	High hydrophobic
Proline	Pro	P		Hydrophilic neural to moderate
Serine	Ser	S	$HOCH_2CH(NH_2)COOH$	Hydrophilic neutral to moderate
Threonine	Thr	T	$CH_3CH(OH)CH(NH_2)COOH$	Hydrophilic neutral to moderate
Tryptophan	Trp	W	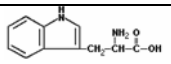	Hydrophilic neutral to moderate
Tyrosine	Tyr	Y	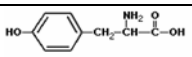	Hydrophilic neutral to moderate
Valine	Val	V	$CH_3CH(CH_3)CH(NH_2)COOH$	Hydrophobic neutral

Table I A List of the 20 natural amino acids. In the first column the abbreviation is present, the letter which is designed each amino acid and his chemical formula is given. At the end column the hydrophilic nature of these amino acids is present.

In all twenty amino acids, except glycine, the carbon atom with the amino group is attached to four different substituents. The tetrahedral bond angles of carbon and the asymmetry of the attachments make it possible for amino acids to have two non-superimposable structures, the L and R forms, which are mirror images of each other. L-amino acids are found in proteins but not always. L-amino acids have the amino group to the left when the carboxyl group is the top, as illustrated in figure 3.

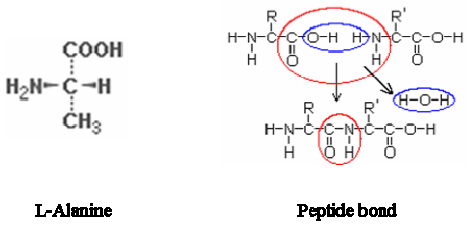

Fig. 3 Reaction of two amino acids, where R and R' are any functional groups from the table above. The blue circle shows the water (H_2O) that is released, and the red circle shows the resulting peptide bond (-C(=O)NH-). The reverse reaction, i.e., the breakdown of peptide bonds into the component amino acids, is achieved by *hydrolysis*.

1.2.1.3 Acid/basic properties

The overall charge on a peptide or protein depends on its amino acid content and, of course, the pH of the solution in which the peptide resides. Simply, the net charge exhibited by a peptide is the sum of the individual charges present on the amino terminus, the carboxy terminus and any ionizable side chains that are present.

The guiding principle in determining the ionization state of an ionizable group is to remember that when the pH of a solution equals the pK_a for an ionizable group, the group is in a 50:50 mixture of its acidic form and the conjugate base. Also, the further the pH of the solution is from the pKa the more the farther the balance between acid and conjugate base is tipped. If the pH is less than the pK_a, then the acid form of the compound predominates. If the pH is greater than the pK_a, then the conjugate base predominates.

Type I groups are neutral in their acidic form (HA); they dissociate to give a proton (H^+) and a conjugate base (A^-) negatively charged:

$$HA \rightleftharpoons H^+ + A^- \quad (1)$$

Thus, type I groups carry a negative charge when pH > pKa. They are neutral when pH < pKa.

Type I groups found in proteins are carboxyl groups (the side chains of aspartate and glutamate, as well as the C-terminus), the sulfhydryl group in the side chain of cysteine and the phenolic side chain of tyrosine.

The acid form (HA^+) of **type II** groups are positively charged and dissociate to form a proton (H^+) and an uncharged conjugate base (A):

$$HA^+ \rightleftharpoons H^+ + A \quad (2)$$

Thus type II groups are uncharged when pH > pK_a and carry a positive charge when the pH < pK_a.

Examples of type II groups found in proteins include *amino groups* (the side chain of lysine and the

alpha-amino group of the N-terminus), the imidazole side chain of histidine, and the guanidinium group of arginine.

1.2.1.4 Proteins

Proteins are large molecules composed of one or more chains of amino acids in a specific order; the order is determined by the base sequence of nucleotides in the gene that codes for the protein.
Proteins are linear heteropolymers of fixed length; i.e. a single type of protein always has the same number and composition of monomers, but different proteins have a range of monomer units, from a few tens to thousand. The monomers are amino acids, and there are 20 types, which themselves have a range of chemical properties. There is therefore a great diversity of possible protein sequences. The linear chains fold into specific three-dimensional conformations, which are determined by the sequence of amino acids; proteins are generally self-folding. The three-dimensional structures of proteins are therefore also extremely diverse, ranging from completely fibrous, to globular.
Protein structures can be determined to an atomic level by X-ray diffraction and neutron-diffraction studies of crystallized proteins, and more recently by nuclear magnetic resonance (NMR) spectroscopy of proteins in solution.

1.2.1.4.1 Protein structure

Experimental structure determination, or structure prediction, helps to the elucidation of protein function; conversely, synthetic protein sequences might be designed so that the protein performs a desired function.

1.2.1.4.1.1 Primary structure

Proteins, like peptides, are composed of amino acids joined together via amide linkages. The only difference between peptides, polypeptides and proteins is the number of amino acid residues in the chain. The relationship between residue count and these terms is somewhat arbitrary. Generally, peptides are small 10 or 20 residues; polypeptides might range up to 50 or 60 residues, with anything larger considered a protein.

1.2.1.4.1.2 Secondary structure

Secondary structure is "local" ordered structure brought about via hydrogen bonding mainly within the peptide backbone.

The most common secondary structures in proteins are the alpha (α) helix and the beta (β) sheet. The backbone of an alpha helix is arranged in a spiral similar to that seen on a cork screw. Notice how the sidechains stick more-or-less straight out from the backbone. The alpha helix is stabilized by hydrogen bonds between the carbonyl oxygen of one amino acid and the backbone nitrogen of a second amino acid located four positions away.

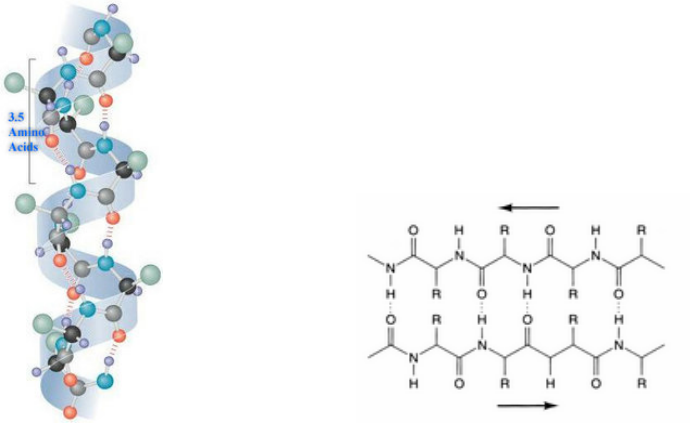

Fugure 4 : A) diagram of the alpha helix structure of amino acids, B) Diagram of B-Pleated sheet and bond structure of protein.

1.2.1.4.1.3 Tertiary structure

The tertiary structure of a protein is its overall shape. All protein molecules are simple unbranched chains of amino acids, but by coiling into a specific three-dimensional shape that they are able to perform their biological function. The tertiary structure that a protein assumes to carry out its physiological role inside a cell is known as the native state or sometimes the native conformation. A protein assumes tertiary structure by "folding". An important type of chemical bond involved in stabilizing the tertiary structure of many proteins is the disulfide bond.

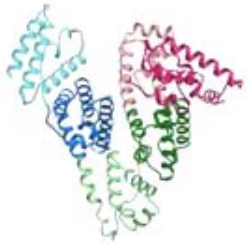

Figure 5: A representation of the 3D structure of human serum albumin (HAS), showing coloured alpha helices. HSA has long been known to be a remarkably flexible molecule

1.2.1.4.1.4 Quaternary structure

Quaternary structure involves the association of two or more polypeptide chains into a multi-subunit structure. Quaternary structure is the stable association of multiple polypeptide chains resulting in an active unit. Not all proteins exhibit quaternary structure. Usually, each polypeptide within a multisubunit protein folds more-or-less independently into a stable tertiary structure and the folded subunits then associate with each other to form the final structure.

Quaternary structures are stabilized mainly by noncovalent interactions; all types of noncolvalent interactions: hydrogen bonding, van der Walls interactions and ionic bonding, are involved in the interactions between subunits. In rare instances, disulfide bonds between cysteine residues in different polypeptide chains are involved in stabilizing quaternary structure.

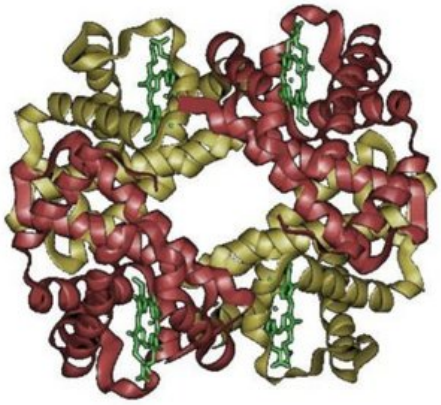

Figure 6: typically quaternary structure, 3-dimensional structure of haemoglobin

1.2.1.5 The polynucleotide: DNA

The nucleotides may be considered as one of the most important metabolites of the cell. Nucleotides are found primarily as the monomeric units comprising the major nucleic acids of the cell, RNA and DNA. However, required for numerous other important functions within the cell.

The fundamental chemical building block of deoxyribonucleic acid (DNA) is the nucleotide. A nucleotide consists of three parts: (1) a nitrogen-containing pyrimidine or purine base, (2) a

deoxyribose sugar, and (3) a phosphate group that acts as a bridge between adjacent deoxyribose sugars. Each deoxyribose sugar unit contains five carbon atoms joined in a ring structure with an oxygen atom. The carbon atoms of the deoxyribose sugar are designated by numbering them sequentially from one to five. The first carbon atom, the 1´ carbon, is by definition the carbon atom covalently attached to one of four organic bases: guanine (G), adenine (A), thymine (T), or cytosine (C). Adenine and guanine are purines, and cytosine and thymine are pyrimidines. Phosphate groups are attached to the third (3´) and fifth (5´) carbon atoms. In DNA, the nucleotide term refers to the complete assemblage of a nitrogenous base (A, G, C, or T), a five-carbon deoxyribose sugar, and a phosphate group (Fig.4).

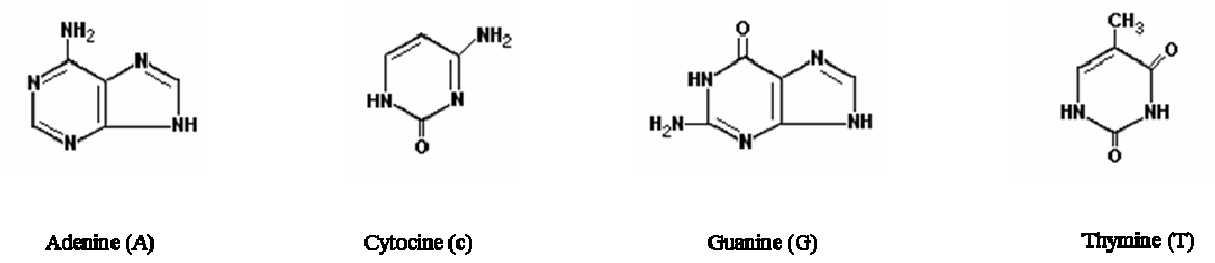

Fig. 7: Chemical structure of the four nucleotides.

The interaction of DNA with nucleic acid binding proteins in transcription and storage, called chromatin, is one example of in vivo association between proteins and polyelectrolytes. DNA is bound to the histones through electrostatic forces between the negatively charged phosphate groups in the DNA backbone and positively charged amino acids (e.g., lysine and arginine) in the histone proteins. Histone proteins are modified by the addition of acetyl, methyl, or phosphate groups, and this alters the strength of the bonding between the histones and DNA. Similar modifications are usually associated with the regulation of biological processes such as DNA replication, gene expression, chromatin assembly and condensation, and cell division.

1.2.2 Synthetic polymers (artificial polyelectrolytes)

The synthetic polyelectrolytes include polymers that can be made by several methods, the major one being chain growth polymerization. The distinctive behavior of polyelectrolytes in aqueous solutions is what separates this class of polymers from non-ionic polymers. In solution, the polymer coils are greatly expanded by the presence of charged groups. If the solution is free of added electrolytes the polymer coil expands as the polymer concentration decreases. This is known as the "polyelectrolyte effect".

1.3 Polyelectrolyte charge classification

By definition, we call polyelectrolyte all macro-molecule that contain a fraction $\boldsymbol{f} < \mathbf{0}$ of ionizable monomers. We can represent it like a **N** monomer chain distributed in **(1-*f*)N** neutral monomers written down as **M** and $\boldsymbol{f}$ **N** represented ionizable monomer written down as $\mathbf{A^-/B^+}$, susceptible to dissociate in $\mathbf{A^-}$ and $\mathbf{B^+}$ (Fig. 8). **M** and $\mathbf{A^-/B^+}$ are chains whit random accommodation.

Two parameters are necessarie to describe a polyelectrolyte:

- **N** : Chain "Length" (number of monomers by chain)
- $\boldsymbol{f}$: total charge, with:

$$\mathbf{0} < \boldsymbol{f} \leq \mathbf{1} \tag{3}$$

Water-soluble polymers can be anionic, cationic, or nonionic depending upon the used monomers. Anionic polyelectrolytes are made by ionizable monomers through the chain with $\mathbf{A^-}$ and cationic polyelectrolytes are the opposite situation (Fig. 8). Nonionic polymers are called Polyampholytes (PA) and contain both positive and negative charged units on the same chain. Proteins and DNA are polyampholytes.

a) Anionic polyelectrolyte:

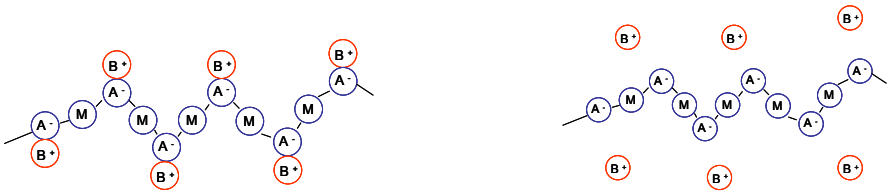

Not dissociated Dissociated

b) Cationic polyelectrolyte

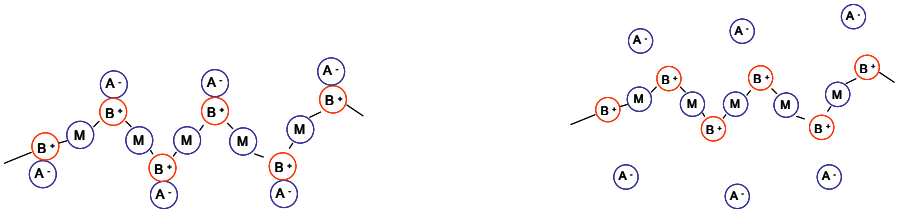

Not dissociated Dissociated

Figure 8: a) Anionic polyelectrolyte non dissociate and in dissociates form. b) cationic polyelectrolyte not dissociated and dissociated form.

Polyelectrolytes can be categorized into two groups: strong polyelectrolytes, for which the degree of ionization is independent of the solution pH, and weak polyelectrolytes, for which the degree of ionization is determined by the solution pH.

1.3.1 Weak and Strong polyelectrolytes

The degree of charge of most polyelectrolytes is controlled by a chemical equilibrium between the charged and uncharged versions of the monomers, which can be tuned by the pH of the solution. Strong polyelectrolytes are typically fully charged whereas weak polyelectrolytes are only partially charged at normal conditions (pH ≈ 7).

Electrostatic repulsion between charges on neighbouring monomers tends to decrease the effective charge of a polyelectrolyte. This effect is stronger at low salt concentrations.

1.3.1.1 Weak polyelectrolytes

A weak electrolyte is a compound that when dissolved in water only partially ionizes or dissociates into ions. That is, the compound exists in water as a mixture of individual ions and intact molecules. The degree of ionization is determined by the solution pH.

$$acid = base + H^+ \qquad K_A = {}^{a}\text{base}{}^{a}\text{H}+/{}^{a}\text{acide} \qquad (4)$$

where a_i determine the activity of *i.*

pH	pK_a -2	pK_a -1	pK_a	pK_a +1	pK_a +2
f	0.01	0.1	0.5	0.9	0.99

In opposite case

pH	pK_a -2	pK_a -1	pK_a	pK_a +1	pK_a +2
f	0.99	0.9	0.5	0.1	0.01

Weak polyelectrolytes:

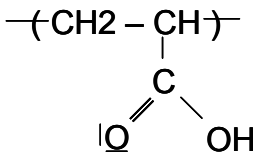

poly (acid acrylic)
PAAH

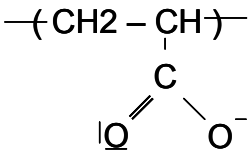

poly (sodium acrylate)
PAANa

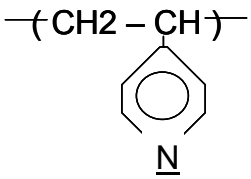

polyvinylpiridine
PVP

1.3.1.2 Strong polyelectrolytes

A strong electrolyte is a compound that when dissolved in water will completely ionize or dissociate into ions. That is, the compound exists in water only as individual ions, and there are no intact molecules at all. Here the degree of ionization is independent of the solution pH.

Strong polyelectrolytes

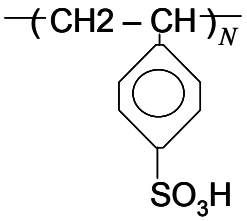

poly (styrenesulfonate)
PSS

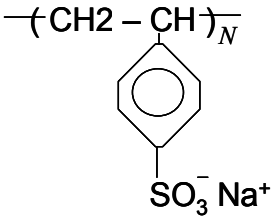

poly (sodium styrenesulfonate)
PSSNa

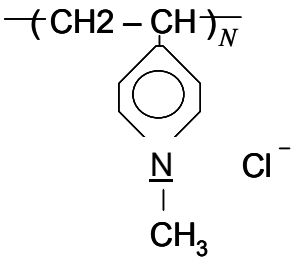

Polyvinylpiridinium
PVPQuat

1.4 Ion dissociation into a solvent

In a homogen environment, the solvent has a relative dielectric constant of ε_r. The cohesion forces between **A-** and **B+**, of valences **ZA** and **ZB** respectively are essentially electrostatic and are determined by the function of the distance between $\mathbf{A}^-$ and $\mathbf{B}^+$**:**

$$F_{A^-/B^+} = \frac{Z_A Z_B e^2}{4\pi\epsilon_r\epsilon_0 r^2_{AB}} \qquad (5)$$

where *e* is the elementary electric charge ($e=1.6 \times 10^{-19}$ C) and ϵ_0 the electric constant of life ($\epsilon_0=8.84\ 10^{-12} C^2N^{-1}m^{-2}$).

The dielectric constant or permittivity (ε) is an index of the ability of a substance to attenuate the transmission of an electrostatic force from one charged body to another. The lower the value the greater will be the attenuation. The standard measurement apparatus utilizes a vacuum whose dielectric constant is 1.

1.4.1 Quality of the solvents

Polyelectrolytes are polymers with groups that dissociatein solution with high dielectric constant (e.g. aqueous solution), releasing counterions into solution and leaving charged monomers on polymer backbons. The intramolecular electrostatic repulsion between charged monomers forces the chain to adopt a certain conformation in solution. The behaviour of polyelectrolytes in solution strongly depends on the solvent quality for polymer backbones.

1.4.2 Polyelectrolyte water behavior classification

Hydrophilic polyelectrolyte

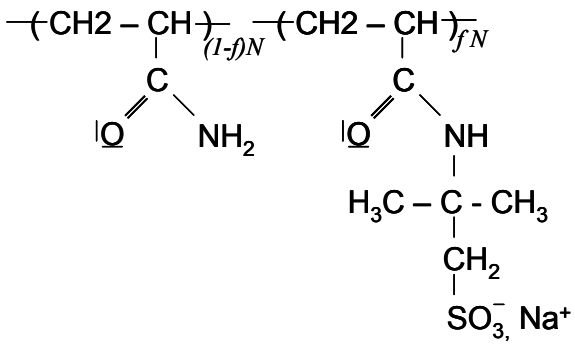

Sudium acrylaminpropansulfonate
AMAMPS

hydrophobic polyelectrolyte

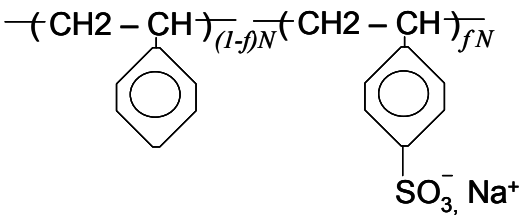

poly (styrenesulfonate)
PSS

1.5 Polyelectrolyte effects

We call polyelectrolyte effects the behaviour of the polyelectrolyte affected by the different factors as concentration, charge of the polyelectrolyte, the hydrophilic nature of the polyelectrolyte, as well as, the ionic strength.

Polyelectrolytes are polymers with ionizable groups that in solution with high dielectric constant (e.g. in aqueous solution) dissociate, releasing caunterions into solution and leaving charged monomers on polymer backbones[1]. Intramolecular electrostatic repulsion between charged

monomers forces chains to adopt elongated conformations in solution. The behaviour of polyelectrolytes in solution strongly depends on the solvent quality for polymer backbones. In a good or Θ- solvent the chain size can be estimated from the balance of the chain elasticity and electrostatic repulsion between charged monomers [2,3]. Polyelectrolyte size increased with increasing fraction of charged monomers on polymers chains. In poor solvent the situation is qualitatively different for polyelectrolytes. The shape of these polymers is determined by the interplay between electrostatic and polymer-solvent interactions. Polyelectrolytes are called hydrophobic when water is a poor solvent for the backbone. As many artificial or natural macromolecules may have some intrinsic hydrophobicity, understanding the behaviour of hydrophobic polyelectrolytes constitutes a difficult area for fundamental and practical physical studies.

Although a full description of polyelectrolytes behaviour in solution is still missing at present, several approaches exist and use different types of approximations and computer simulations.

This section will give a general overview of the main theoretical approximations that has been proposed to understand the behaviour of polyelectrolytes in solution free of ions, as well as, with ion strength. Finally we will revise the main theoretical approximations proposed for polyelectrolytes adsorption in charged substrates.

1.6 General behavior of polyelectrolytes in solution

The first theoretical model for the conformation of an individual weakly charged polyelectrolyte molecule in a poor solvent was proposed by Khokhlov[4]. This model suggests that, due to the balance between the electrostatic repulsion and globule's surface tension, the chain forms an elongated cylinder. However, the cylindrical globule is unstable with respect to capillary wave fluctuations, which cause a splitting into spherical collapsed cores and extended strings. The equilibrium intrachain tension in the string is determined only by the solvent ionic strength, i.e., by the strength of the short range attraction between the monomers. This instability was first shown for a neutral polymer subjected to an external extensional force in a poor solvent[5,6]. Later it was realized that it also occurs for charged chains, where the extension is caused by the intramolecular Coulomb repulsion [7,8]. For the connectivity of the monomers, one can expect the formation of a necklace type structure in which the collapsed spherical beads are connected by extended narrows strings whose tension balance the Coulomb repulsion. This unusual conformation was obtained theoretically by Dobrynin *at al.*[9] by analogy with the Rayleigh instability of a charge droplet[7]. It

focuses on the essential features, which are short-range attraction (poor solvent condition) and long-range repulsion (unscreened Coulomb interactions in a salt-free solution) between monomers connected to a chain. In fact a neutral hydrophobic polymer when immersed in water forms spherical globule (like a drop of oil in water) in order to minimize the interfacial area with the solvent. When charges are added to the polymer the associated electrostatic energy of the globule increases until it balances the interfacial energy at some critical charge fraction f_c. Beyond f_c the globule splits into two smaller ones thus increasing the interfacial area but decreasing the electrostatic energy. Contrary to the case of a charged droplet, the presence of connected monomers hinders infinite separation and elongated string is formed between the pearls. Therefore the resulting structure is a water-soluble pearl-necklace composed of dense pearls connected by narrow string[10]. The size of the pearls is determined by the balance between electrostatic and surface tension. The distance between two pearls is governed by the balance of the electrostatic pearl-pearl repulsion and the surface tension. Theoretical prediction has been confirmed by simulations using the Debye-Hückel approximation[11], and with explicit counterions[12]

Experimentally, Essafi[13] studied PSS, as a model hydrophobic polyelectrolyte. By measuring the fluorescence emission of pyrene probes they observed the existence of low dielectric constant nano-regions dispersed along chains in agreement with the presence of hydrophobic pearls on the chains. The most important theories will be revised in the following sections.

1.6.1.1 Structure of hydrophobic polyelectrolytes in poor solvents

The most spectacular property of hydrophobic polyelectrolytes is the pearl-necklace conformation predicted for the single chain. This unusual conformation was obtained theoretically by Dobrynin by analogy with the Rayleigh instability of a charged droplet.

Kantor and Kardar[7] have recently proposed that a polymer with a short-range attraction and long-range repulsion may form a necklace with compact beads joined by narrow strings. Dobrynin[8] extended this idea and developed a scaling theory that describes how, with varying solvent quality or charge on the chain, the polyelectrolyte in a poor solvent undergoes a cascade of abrupt transitions between necklace-like configurations with different number of beads.

Consider a dilute polyelectrolyte solution of chains with the degree of polymerization N, monomer size b, and fraction f of charged monomers in a poor solvent with dielectric constant ϵ. An uncharged chain in a poor solvent forms a globule. The monomer density $\rho \approx \tau / b^3$ inside this

globule is defined by the balance of the two-body attraction ($bN\rho$) and the three-body repulsion ($b^2N\rho^2$) between the monomers of the chain. The size R of the globule with density ρ is equal to:

$$R \approx (N/\rho)^{1/3} \approx b\tau^{-1/3}N^{1/3} \tag{6}$$

If the polymer is charged, the Coulomb repulsion between charged monomers could change the shape of the globule, but would not significantly affect its volume. The volume occupied by the molecule is still defined by the solvent quality, as in the case of uncharged globule. If the Coulomb repulsion $F_{Coul} \approx e^2 f^2 N^2/\epsilon R$ (here e is elementary charge) becomes comparable to the surface energy $F_{sur} \approx kTR^2/\xi_T^2$, the total energy of the globule can be lowered either by elongating it into a cylinder or by splitting into two smaller globules connected by a narrow string. This deformation occurs when the total valence of the charge fN becomes larger than $(N\tau/u)^{1/2}$. Here $u \approx l_B/b$ is the ratio of the Bjerrum length $l_B = e^2/\epsilon kT$ to the bond length b.

1.6.1.2 Necklace Globule

The problem of the shape of charged globule is similar to the classical problem of the instability of a charged droplet, considered by Rayleigh. He show that a spherical droplet with radius R and charge $Q > \epsilon(\gamma R^3 / kTl_B)^{1/2}$ (were γ is a surface tension) is locally unstable and will spontaneously deform. The equilibrium state of this system is a set of small droplets with the charge on each on them lower than the critical one and placed at an infinite distance from each other. This final state is impossible for the charged polymer because it consist of monomers connected into a chain by chemical bonds. In this case, the system can reduce its energy by splitting into a set of smaller charged globules connected by narrow strings-the necklace globule, as it was called by Kantor and Kardar.

1.6.1.3 Monte Carlo simulation

Monte Carlo Simulations of polyelectrolytes in poor solvents are used to validate these predictions. Consider a freely joined uniformly charged chain consisting of N monomers with charge fe on each[14]. The monomers interact with each other through a Coulomb potential:

$$\frac{U_{Coul}(r_y)}{kT} = \frac{ubf^2}{r_y} \tag{7}$$

and a Lennard-Jones potential

$$\frac{U_{LJ}(r_{ij})}{kT} = \epsilon_{LJ}\left[\left(\frac{r_0}{r_{ij}}\right)^{12} - 2\left(\frac{r_0}{r_{ij}}\right)^{6}\right] \tag{8}$$

Where $r_{ij} = |r_i - r_j|$ is the distance between the *i*th and *j*th monomers. The Lennard-Jones potential has its minimum value $-kT\,\epsilon_{LJ}$ at distance $r_{ij}=r_0$ (where r_0 is equal to the bond length *b*). The results obtained from the simulation show that at a low valence $f < 1.7/N$ chain forms spherical globules (Figure 10a) with a size proportional to *N*. When the charge density becomes longer than the critical value f 1.7 / *N* the polyelectrolyte takes a dumbbell configuration (Figure 10b). At still higher charge density, the polymer can form a necklace configuration of three beads joined by two strings (fig.10c). These results of the Monte Carlo simulation support the prediction of the necklace configuration of polyelectrolytes in poor solvents proposed by Dobrynin.

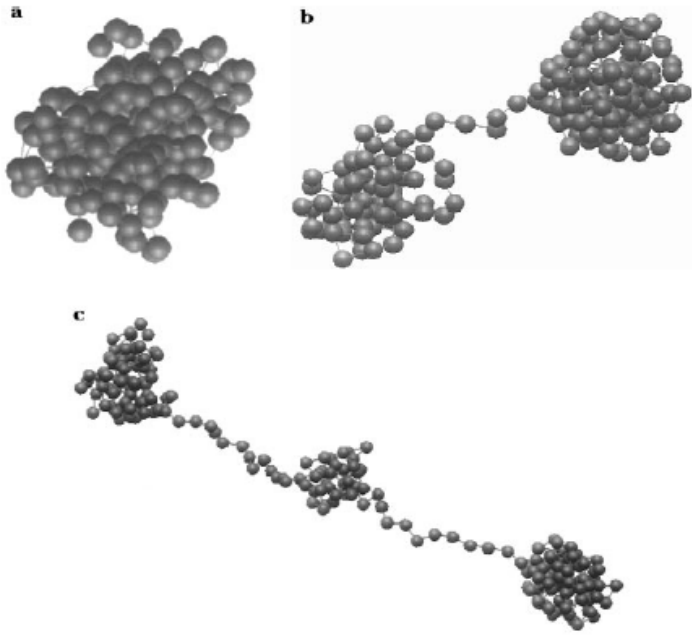

Figure 10. Typical configurations of a freely jointed uniformly charged chain with *N*) 200 monomers interacting via Coulomb and Lennard-Jones potentials (with _LJ) 1.5 and *u*) 2) at three different charge densities: (a) spherical globule for *f*) 0; (b) dumbbell for *f*) 0.125; (c) necklace with three beads for *f*) 0.15 (Ref. 8).

In other hand, the prediction can also be tested by small-angle neutron (SANS) or small-angleX-ray (SAXS) scattering experiments. The scattering function of the polymer solution containing the necklace globules is:

$$S(\mathbf{q}) \approx n_s \langle \sum_{i,j} \exp(-i(\mathbf{r}_i - \mathbf{r}_j)) \rangle_a \tag{9}$$

Where brackets $\langle\rangle_a$ denote averaging over all macromolecular orientations, is the number of macromolecules per unit volume in dilute solution or the density number of chain sections of the size of the correlation length in semidiluted solutions. Summation in above equation is carried out

over all monomers of a given chain (or section of chain). If the necklace contains N_{bead} beads of size D with m_{bead} monomers in each joined by string l_{str}, then after averaging over all chain orientations, the scattering function can be rewritten as:

$$S(\mathbf{q}) \approx n_s m_{\text{bead}}^2 \left\{ N_{\text{bead}} + 2 \sum_{n=1}^{N_{\text{bead}}-1} (N_{\text{bead}} - n) \times \frac{\sin(q l_{\text{str}} n)}{q l_{\text{str}} n} \right\} \left\{ \frac{\sin(qD) - qD\cos(qD)}{(qD)^3} \right\}^2 \tag{10}$$

These experiments are consistent in the prediction above present, but detailed experiments are necessary for more quantitative test of this prediction.

In summary this prediction demonstrated that the free energy of these necklace states is much lower that that of a cylindrical globule. The length of the necklace L_{nec} is longer than the length L_{cyl} of the cylinder by the same factor. These result are in agreement with the Monte Carlo Simulation and are consistent with the results of SANS and SAXS experiments on solution of PSS (poly(sterenesulfonate))[15].

1.6.1.4 Ionic strength effect on polyelectrolytes conformation in solution

Electrostatic interactions constitute a key for understanding interactions between charged macroions in ionic solutions. For example, the stability of colloidal particles dispersed in a solvent can be explained by considering the competition between repulsive electrostatic interactions and attractive Van der Waals interactions.

Furthermore, strong (unscreened) electrostatic interactions tend to rigidify flexible objects such as charged polymers (polyelectrolytes). Another characteristic of ions in solutions is that due to entropic effects, temperature is an important parameter controlling equilibrium properties.

Electrostatic forces constituted an important contribution to the interaction between macromolecules in aqueous solution. Two macromolecules with like charge would naturally be expected to repeal each other. The theories of electrostatic interactions between macroions the Poisson-Boltzmann (PB) theory on two parallel cylinders with the same line charge should always repeal each other.

1.6.1.4.1.1 Poisson-Boltzmann equation

The relation between the electric potential ψ (r) and the charge distribution ρ(r) at any point r is given by the Poisson equation

$$\nabla^2\psi = -\frac{4\pi}{\varepsilon_w}\,\rho(\vec{r}) = -\frac{4\pi e}{\varepsilon_w}\,(z_- n_- + z_+ n_+) \tag{11}$$

where $\epsilon_w \approx 80$ is the dielectric constant of the aqueous solution taken as constant within the fluid.
The Poisson equation determines the electric potential for a given spatial charge distribution. However, even for a fixed surface charge distribution, the ions in solution are mobile and can adjust their positions. Consequently, each ion density in the solution obeys a Boltzmann equation according to the electric potential

$$n_i = n_0^{(i)} \mathrm{e}^{-ez_i\psi/T}. \tag{12}$$

The combination of these two equations results in the Poisson-Boltzmann equation which determines the potential ψ self-consistently

$$\nabla^2\psi(\vec{r}) = -\frac{4\pi e}{\varepsilon_w}\left(z_+ n_0^{(+)} \mathrm{e}^{-ez_+\psi(\vec{r})/T} + z_- n_0^{(-)} \mathrm{e}^{-ez_-\psi(\vec{r})/T}\right). \tag{13}$$

Generally, the Poisson–Boltzmann theory is a good approximation in most physiological conditions, especially for monovalent ions and for surface potentials which are not too large. Close to the charged surface, the finite size of the surface ionic groups and that of the counterions leads to deviations from the Poisson–Boltzmann results.

The assumptions which led to the derivation of the Poisson–Boltzmann equation can be summarized as follows: the ionic charge distributions are smeared out and are represented as smoothly varying functions. The discrete nature of the ions is not taken into account and no other molecular interaction between the ions and solvent molecules (water) is considered.
Moreover, the Poisson–Boltzmann theory does not take into account any charge-charge correlations. Physical observables like the charge distributions are replaced by their thermal averages and, in this sense, resemble mean-field results. However, there are experimental and numerical evidence of attractive electrostatic interaction between like charges in polyelectrolyte systems.

1.6.1.4.1.2 Debye-Hückel Theory

An extension of the Poisson–Boltzmann theory including effects of charge images and ion correlations has been developed for counterions (no-added electrolyte) and for symmetric

electrolytes. A linearized form proposed by Debye and Hückel (1923) has been commonly used in practical applications of the PB equation.

$$\nabla^2\phi = \kappa^2\phi, \tag{14}$$

Were $1/_k$ is the Debye screening length given by

$$\frac{1}{\kappa} = \sqrt{\frac{\epsilon_0 \epsilon kT}{2e^2 n_0}}. \tag{15}$$

It varies from about 3 Å for a 1M of electrolyte like NaCl to about 1 μm for pure water (due to the ever presence of H+ and OH− ions even in pure water with an ionic strength of about 10^{-7} M). In the presence of a relatively strong electrolyte, the electrostatic interactions are exponentially screened and can be effectively neglected for lengths larger than the Debye–Hückel screening length λ_D.

Finally the PB equation and the Debye-Hücke screening length λ_D can be rewritten as:

$$\nabla^2 < \phi(\mathbf{r}) > = \frac{e^2 \sum_i z_i^2 n_i^{(0)}}{\epsilon_0 \epsilon KT} < \phi(\mathbf{r}) > . \tag{16}$$

1.6.1.5 Polyelectrolyte domains formation in solution

In the other hand Sedlak[16] found experimentally by dynamic light scattering, submicron size domains of polyelectrolyte in solutions. The presence of domains was reflected in small-angle neutron scattering (SANS) data too[17,18]. These particles are substantially bigger compared to ion-containing polymers and hence also the distances at which interactions work are much larger. The analogy is, however, evident. Many experimental results in this field cannot be also explained on the basis of purely repulsive interactions between macroions. One important experimental finding was the observation that light scattering was influenced by the filtration procedure performed prior to measurement, when fine filters with submicron pore sizes comparable with domain dimension were used[19].

Domains can coalesce upon pressure filtration as well as break into smaller ones. Retention based on the size exclusion cannot be completely excluded but it does not represent the main mechanism. Natural size distribution of domains (size distribution without filtration procedure) was also investigated. It was found that the size distribution is relatively extensive. Domains sizes in one

sample may range from approximately from 40nm up to 400nm and the presence of even smaller domains cannot be exclude, but cannot be quantitatively estimated by a limited range of experimentally accessible scattering vector.

The natural size distribution calculated by light scattering data was verified by filtration trough a set of filters with different pore sizes. Results of these experiments agree with the calculated size distribution. The natural size distribution of domains is not a unique stable state to which the system would spontaneously return after filtration. No spontaneous growth or coalesce of smaller domains into larger ones, which are usually present in solution prior to filtration, was observed by Sedlak.
Filtration in general is a routine purification procedure used for polyelectrolytes. Results of this work show that this procedure has substantial influences on the experimental data on domains and it is necessary to know how.
Finally, most polyelectrolytes theories assume that the ions responsible for creating the ionic atmosphere around the macroions can be treaded as point charges. If this assumption is true, then a whole layer of potential difficulties involving ion species, and discrete vS continuum effects can be avoided. Early reports of ionic specificity in polyelectrolytes by Flory and Osterhed[20], in presence of different salts NaCl, $CaSO_4$ and $CaCl_2$ demonstrated that changing the anion in monovalent salts had little effect but when the valence was changed from monovalent to divalent the effects were much larger, suggesting a purely electrostatic effect. They describe the differences between the ion species of the same valence in terms of the activity of the ions near the polyelectrolyte. Other, even more dramatic ion specific effect occur when DNA is exposed to multivalent ions[21,22]. DNA is condensed into a torus shape when exposed to multivalent ions as spermine, $Co(NH_3)_6$, or even divalent ions in mixed alcohol/aqueous solution[23]. There are first-order differences in polyelectrolyte conformations, interactions, and hydrodynamics when electrolytes of different valence and symmetry are added to the polyelectrolyte solution. Second order effect in these properties are seen when the chemical identity of the anions is changed for a given symmetry and valence class, and yet weaker second-order effects are seen when changing the cation in a given class. These effects can be resuming in specific condensation and collapse phenomena[24].

1.7 Adsorption of hydrophobic polyelectrolytes at oppositely charged surfaces

The adsorption of polyelectrolytes onto oppositely charged surfaces driven by Coulomb attractive forces has been a classical problem in polymer physics over two decades. In the pioneering paper of

Wiegel[25], the adsorption of an individual chain was considered in absence of any interactions other than the electrostatic attraction of the charged monomers to the surface described by a screened Coulomb or Debye-Hückel potential. In real solutions, in addition to the polyelectrolyte-surface attraction there is a hierarchy of interations (intra and inter-chain) that affect significantly the adsorption. Attempts to take these interactions into account were made[26,27,28].

The conformation of polyelectrolytes in a poor solvent adsorbed onto an oppositely charged interface is determined by the balance of i) the electrostatic attraction of the charged monomers to the surface; ii) intra-chain Coulombic repulsion between charged monomers; iii) the surface free energy of the deformed globule interface. Both the Coulombic interaction between the chain and the interface and the intra-chain Coulombic repulsion are screened by addition of salt in solution and by the localization of the counterions near the strongly charged surface. Adsorption can be induced either by increasing the surface charge density or by decreasing the ionic strength of the solution.

The conformation of an adsorbed chain in the globular state leads to flat pancakes on the surface. This is very similar to the flattening of a liquid drop on a solid surface under the influence of gravity. For an adsorbed polyelectrolyte necklace, an increase of the ionic strength of the solution results first in the coalescence of compressed beads into a uniform pancake and then to desorption. An increase in the surface charge density, at low ionic strength, result in the compression of adsorbed globular beads, and (at sufficiently low ionic strength) in the coalescence of the beads to form a uniform pancake[29].

In practice, the number of pearls is not always very large (as seen in several numerical simulations) and the discreteness of the pearls becomes an important factor. For two pearls, when the external force is increased, a well-defined metastable single string state appears in addition to the two-pearl necklace. For a higher force, the single string and the two-pearl necklace exchange stability. At this critical force, the pearl size is still close to the pearl size in absence of external forces. When about half of the pearls are unwinded, the metastable two-pearls state disappears and the single-string state is the only equilibrium conformation. For a fast stretch-collapse cycle, a hysteresis loop describing most of the metastable branches is expected.

For necklaces containing more pearls, the intensive string properties, tension, etc. are kept constant and the only variables which are allowed to fluctuate are the number of monomers in a pearl and the

number of pearls; this allows a transfer of the monomers from the pearls towards the strings as the applied force is increased. In this model the number of pearls to be bound is an integer[30].

1.7.1 Substrates

In the first approach, suitable support materials must carry a minimal surface charge. If the surface of the surface is brought into contact with the solution of polyion of opposite charge, the first polymer layer is adsorbed and adheres.
The choices of substrates have so far been dominated by their convenience for particular analytical methods. Glass, quartz, silicon, wafers, mica and gold coated supports are materials most frequently used.

All the above mentioned materials are additionally characterized by the simplicity with which charge groups can be created on the surface. The surface of cleaved mica sheets are inherently negatively charged in water, due to the dissociation of the potassium cations of this alumsilicate in water. The silanol groups at the surface of glass and quartz, as well as of silicon wafers due to the thin surface layer of oxide, can by easily deprotonated by base. Treatment with various functionalized silanes provides an additional, easy access to positively charged surfaces. In a similar way, treatment of gold with functionalized thiols or disulfides, respectively, enable the tailoring of both positively or negatively charged surface.

When a substrate is treated with polyelectrolytes, each polyelectrolyte deposition cycle generates a new substrate. The film growth is characteristic for a chosen pair of polyelectrolytes and its "matching", and on the conditions for adsorption. Therefore, it is not surprising that the amount of a given polyelectrolyte which is adsorbed during the first deposition cycle depends on the substrate used and its surface treatment. Typically, the amount of adsorbed polymer per deposition cycle increases during the initial 1 to 5 deposition cycles, and then approaches a constant value. In parallel, the average chemical composition of the surface becomes constant. If poorly charged surfaces are used, this transition regime can stretch even over much more than five deposition cycles.

However finally, constant growth is obtained for a well behaving polyelectrolyte pair. In this regime, the thickness per layer pair is characteristic for polyelectrolytes employed and conditions applied (polyion concentration, ionic strength, rinsing and drying steps etc., see below). Most

studies found that this thickness increment is independent of the chemical nature of the support. However in a few cases, the thickness per layer pair was reported to depend on the detailed nature of the support even during stable multilayer growth. We have never encountered such a phenomenon in our studies. Even for so different supports such as quartz and untreated polypropylene, we observed a constant slope in the regime of regular film growth.

Basically, surface modification may provide charges to any substrate, not only to organic polymers, to render it useful for sequential adsorption of polyelectrolyte films (SAPF).

1.7.1.1 Polyelectrolyte-substrate interaction

Theoretical descriptions of polyelectrolyte adsorption take into account the multitude of different interactions and length scales. Among others they include electrostatic interactions between the surface, monomers and salt ions, excluded-volume interactions between monomers and entropy considerations.

Many types of charged molecules and nanoobjects seem to be suitable for deposition by the SAPF method, but mostly polyelectrolytes have been employed. Typically, a solid support with a charged surface is exposed to the solution of a polyion of opposite charge for a short time. The practical set-up may be extremely simple, e. g. just dipping the support into beakers filled with the polymer solutions. The dipping can be done manually, although automatic dipping devices may provide some better control.

The method is relatively rapid, as adsorption steps last typically between 1 min and 1 h. The amount of adsorbed material is self-limiting. The surplus polymer solution adhering to the support is removed by simple washing. Under proper conditions, polymeric material with more than the stoichiometric number of charges (relative to the substrate) is adsorbed, so that the sign of the surface charge is reversed. In consequence, when the substrate is exposed to a second solution containing a polyion of opposite charge, an additional polyion layer is adsorbed. But this reverses the sign of the surface charge again. Consecutive cycles with alternating adsorption of polyanions and polycations result in the stepwise growth of polymer films.

So far, aqueous solutions have been preferred for SAPF, though organic solvents may be equally useful. The method is well suited for automation and has no inherent restriction with respect to form

and size of the substrates. Due to multiple electrostatic interactions between the polymers and to the substrate, the films show normally excellent cohesion, as well as adhesion to the substrate.

1.8 Conclusion

Polyelectrolytes are polymer chains containing a variable amount of ionisable monomers. Once dissolved in a polar solvent such as water, the ion pairs dissociate. The electrostatic charge of one sign is localized on the chain whereas the large number of oppositely charged counterions are scattered in the solution.

Polyelectrolytes are everywhere around us. Most biopolymers, including DNA and proteins, are polyelectrolytes and many water soluble polymers of industrial interest are charged. Thus phenomena specific to polyelectrolytes have strong applications in molecular and cell biology as well as technology.

Despite more than 50 years of continuing investigation, the unique properties of charged polymers are still poorly understood, in contrast to their neutral counterparts. The complexity stems primary from the simultaneous presence of long range electrostatic interactions and short range excluded volume interactions and to the crucial role of counterions.

Aqueous solutions containing polyelectrolytes and small ions are abundant in biological systems, and have been the subject of extensive research in recent years. When such a solution is in contact with an oppositely charged surface, adsorption of the polyelectrolyte chains can occur. Theoretical descriptions of polyelectrolyte adsorption take into account the multitude of different interactions and length scales. Among others they include electrostatic interactions between the surface, monomers and salt ions, excluded-volume interactions between monomers and entropy considerations. Although a full description of polyelectrolytes is still lacking at present, several approaches exist and use different types of approximations.

Experimental studies have shown that adsorbing polyelectrolytes (PEs) may carry a charge greater than that of the bare surface, so that the overall surface polyelectrolyte complex has a charge opposite to that of the bare charged surface. This phenomenon is known as overcharging (or surface charge overcompensation) by the PE chains. When the overcharging is large enough to completely reverse the bare surface charge, the resulting charge surplus of the complex can be used to attract a second type of polyelectrolyte having an opposite charge to that of the first polyelectrolyte layer.

Eventually, by repeating this process, a complex structure of alternating layers of positively and negatively charged polyelectrolytes can be formed.

1.9 Bibliography

[1] *Polyelectrolytes*; Hara, M., Ed.; Marcel Dekker: New York, **1993**.

[2] Khokhlov, A. R. ; Khachaturian, K. A. *Polymer* **1982**, 23.

[3] Dobrynin A. V. ; Colby R. H. ; Rubinstein, M. *Macromolecules* **1995**, 28, 1859.

[4] Khokholov A. R., *J.Phys A*., **1980**, 13, 979.

[5] Halperin A., Zhulina E.B., *Macromolecules*, **1991**, 24, 5393.

[6] Halperin A. Zhulina E B. Europhys Lett. 1991, 15, 417.

[7] Kantor Y. Kardar M. Europhys. Lett. 1994, 27, 5393.

[8] Dobrynin A V, Rubinstein M, Obukhov SP. Macromolecules, 1996, 29, 2974.

[9] Dobrynin A.V. and Rubinstein M. *Macromolecules*, 1999, 32, 915.

[10] Baigli D, Sferraza M, Williams CE. Europhys. Lett. 2003, 11;315.

[11] Lyulin A.V., Dünweg B., Borisov O.V. and Darinskii A.A. *Macromolecules,* **1999**, 32, 3264

[12] Mcka U., Holm C., and Kremer K, *Langmuir*, **1999**, 15, 4033.

[13] Eassafi W., Lafuma F. and Williams C.E., *J. Phys. II*, **1995**, 5, 1269.

[14] Baumgartner AJ. . Chem. Phys. 1980, 72, 871.

[15] Williams C, Wafa E. J. Phys. II 199, 5, 1269

[16] Sedlak M., *J. Chem. Phys*., **2002**, 116, 5236.

[17] Matsuoka H., Schwahn D., and Ise N., *Macromolecules*, **1991**, 24, 4227.

[18] Ermin B.D., and Amis E.J., *Macromolecules*, **1997**, 30,6937.

[19] Sedlak M., *Macromolecules,* **1993**, 26, 1158.

[20] Flory P.J., Osterheld J.E., *J. Phys. Chem*., **1959**, 58, 653.

[21] Osterberg R., Persson D., and Bjursell G., *J. Biomol. Struc. Dyn*., **1984**, 2, 285.

[22] Bloomfield V.A., Willson R.W., and Rau D.C., *Biophys. Chem.,* **1980**, 11, 339.

[23] Gelbart W.M., Bruinsman R.F., Pincus P.A., and parsegian V.A., *Phys. Today*, **2000**, 38.

[24] Sorci G.A., and Reed F.W., *Macromolecules*, **2004**,37, 554.

[25] Wiegel F.W., *J. Phys. A*, **1976**, 19, 299.

[26] Borisov O.V., Birshtein T.M., Zhulia E.B., *J. Phys. II*, **1994**, 4, 913.

[27] Yamakov V., Dünweg B., Borisov O.V., Milchev A., *J. Phys. Condens. Matter*, **1999**, 11, 9907.

[28] Zhulina E.B.,Borisov O.V., van Male J., Leer-makers F.A.M., *Langmuir*, **2001**, 17, 1277.

[29] Borisov O.V., Hakem F., Vilgis T.A., Joanny J-F. and Johner A., *The European Phis. J. E*, 2001, 6,37.

[30] Vilgis T.A., Jhoner A., and Joanny J.F., *The European Phys. J. E*, **2000**,2,289.

Chapter II

2 Materials and Methods

Chapter II **38**
2 Materials and Methods **38**
2.1 Introduction **39**
2.2 AFM Microscope **39**
2.2.1 Piezoelectric ceramic transducer *40*
2.2.2 Operate modes *41*
2.2.2.1.1 Image display 42
2.2.3 Principle *42*
2.2.3.1 Tip-sample interaction mode *42*
2.2.4 Experimental method *43*
2.3 Micro-peeling aspiration technique **44**
2.3.1 Quantification of Cell Adhesion *44*
2.3.2 Experimental method *46*
2.4 Transmission electron microscope **48**
2.4.1 Experimental method *48*
2.5 Ultra violet spectroscopy **48**
2.5.1.1 Fluorescence *49*
2.5.1.2 Intra-molecular redistribution of energy between possible electronic and vibrational states *49*
2.5.1.3 Chemiluminescence *50*
2.5.2 Experimental method *50*
2.6 Materials **50**
2.6.1 Polyelectrolytes *50*
2.6.2 Polyelectrolyte nanorings formation method *51*
2.6.3 Nanoparticles synthesis *52*
2.6.3.1 Experimental method *52*
2.7 Bibilography **53**

2.1 Introduction

Alternating adsorption of anionic and cationic polyelectrolytes on solid surfaces allows the formation of multilayer polyelectrolyte films and constitutes a versatile technique to modify surfaces. During preparation of these polyelectrolytes films, various structures at the surface can be generated. They can not be detected with the optical systems commonly used, in this case the adsorption alteration of cationic and anionic polyelectrolytes on solid surfaces can be studied by AFM microscope, transmission electron microscope, and optical techniques, as wave guide spectroscopy, UV.vis spectroscopy, and dynamic light scattering, are used in order to characterized this surfaces. Also, streaming potential and micro-peeling aspiration technique, are techniques that helps to understand the different parameters studied in this work. The following section covers the basic concepts of these techniques, as well as the full description of materials and methods used.

2.2 AFM Microscope

Microscopes have historically been tools of great importance in biological science. The atomic force microscope (AFM) is one of the family of scanning probe microscopes which has grown steadily since the invention of the scanning tunnelling (ST) microscope by Binnig and Rohrer in the early eighties for which they received the Nobel Prize for Physics in 1986.

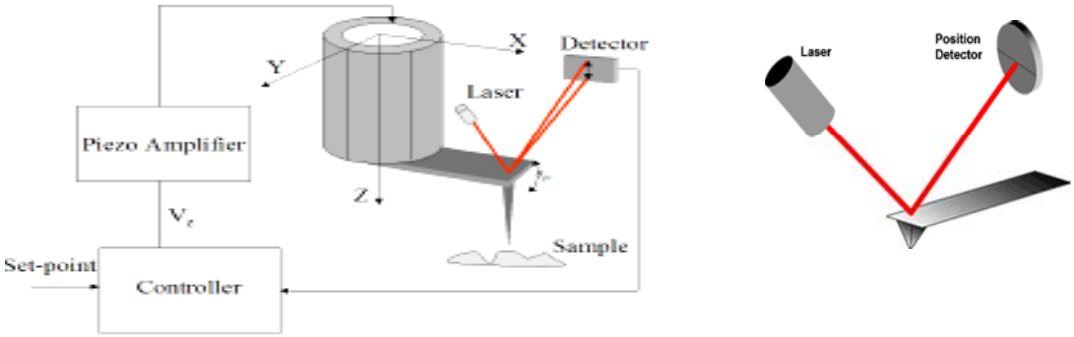

Figure 1 The diagram illustrates how AFMs works; as the cantilever flexes, the light from the laser is reflected onto the split photo-diode. By measuring the difference signal, changes in the bending of the cantilever can be measured.

If the Cantilever obeys Hooke's Law to be given for small displacements, the interaction force between the tip and the sample can be found. The movement of the tip or sample is performed by an extremely precise positioning device made from piezo-electric ceramics, most often in the form of a tube scanner.

The scanner is capable of sub-angstrom resolution in x, y and z directions. The z-axis is conventionally perpendicular to the sample.[1]

2.2.1 Piezoelectric ceramic transducer

The mechanical motion in AFM is created from electrical energy with electromechanical transducer. The electromechanical transducer used in an atomic force microscope is the piezoelectric ceramic.

Piezoelectric ceramic are a class of materials that change in geometry (expand or contract) when it is placed in a voltage gradient or, conversely, create a voltage gradient when forced to expand or contract[2]. The amount of motion and direction of motion depends on the type of piezoelectric material, the shape of material, and the field strength.

Figure 2A shows the motion of a piezoelectric disk when exposed to an electric potential. A typical piezoelectric material will expand by about 1nm per applied. Thus, to get larger motions it is common to make piezoelectric transducer with hundreds of layers of piezoelectric materials (Fig.2B).

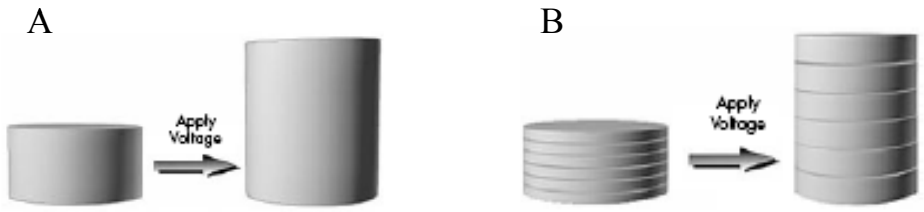

Figure 2 A)when a voltage is applied to the top and bottom surface of the piezoelectric disc, the disc will expand. B) piezoelectric transducer is commonly made by hundreds of layers of piezoelectric materials

By using one thousand layers of piezoelectric material it is possible to get motions as large as 1000 nm per volt. Thus with 100 volts it is possible to get 0.1mm of motion with a multiple layer piezoelectric transducer. Most scanned-probe microscopes use tube-shaped piezoelectric ceramic transducer, which combine a simple one-piece construction with high stability and large range motion.

Four electrodes cover the outer surface of the tube, while a single electrode covers the inner surface. Application of voltages to one of the electrodes causes the tube bend or stretch, moving the sample in three dimensions (X,Y, and Z).

2.2.2 Operate modes

The AFM can be operated in two principal modes

- with feedback control ("Z")
- without feedback control ("error")

If the electronic feedback is switched on, then the positioning piezo which is moving the sample (or tip) up and down can respond to any changes in force which are detected, and alter the tip-sample separation to restore the force to a pre-determined value. This mode of operation is known as constant force, and usually enables a fairly faithful topographical image to be obtained (hence the alternative name, height mode).

If the feedback electronics are switched off, then the microscope is said to be operating in constant height or deflection mode ("error", see figure 3). This is particularly useful for imaging very flat samples at high resolution. Often it is best to have a small amount of feedback-loop gain, to avoid problems with thermal drift or the possibility of a rough sample damaging the tip and/or cantilever. Strictly, this should then be called error signal mode.

The error signal mode may also be displayed whilst feedback is switched on; this image will remove slow variations in topography but highlight the edges of features.

Alternative image can be obtained when measure of friction between tip and sample are take. If the scanner moves the sample perpendicular to the long axis of the cantilever (Fig.4), friction between the tip and sample causes the cantilever to twist. A photo detector position-sensitive in two dimensions can distinguish left and right motion of the reflected laser beam from the up and down motion caused by topographic variants.[3]

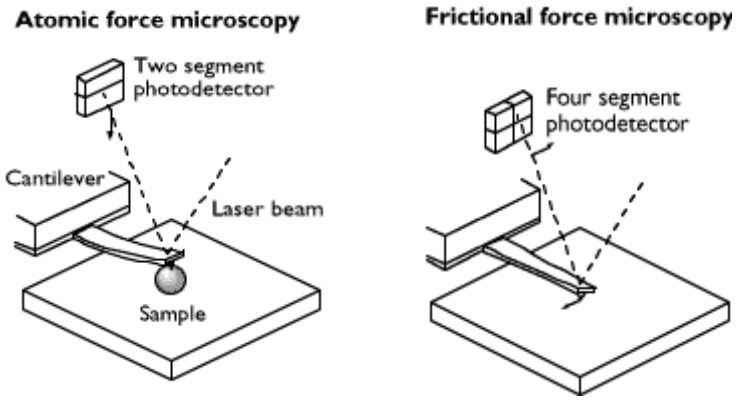

Figure 3: While topographic imaging uses the up-and-down deflection of the cantilever (left), friction imaging uses torsional deflection (right).

Therefore, AFMs can measure tip-sample friction while imaging sample topography. Besides serving as an indicator of sample properties, friction (or lateral force, or lateral deflection) measurements provide valuable information about the tip-sample interaction.

In most AFMs microscopes is possible to get the different modes at the same time.

2.2.2.1.1 Image display

Height image data obtained by the AFM is three-dimensional. The usual method for displaying the data is to use a color mapping for height, for example black for low features and white for high features.

2.2.3 Principle

The theory and operation of an atomic force microscope is similar to a stylus profiler. The primary difference is that the atomic forces microscopes, the probe force on the surface are much smaller than those in a stylus profiler. Because the forces in AFM are much smaller, smaller probes can be used, and resolution is much higher than can be achieved with a stylus profiler[4].

2.2.3.1 Tip-sample interaction mode

Three main classes of tip-sample interaction can bee used: contact mode, tapping mode and non-contact mode.

Contact mode is the most common method of operation of the AFM. As the name suggests, the tip and sample remain in close contact as the scanning proceeds. By "contact" we mean in the repulsive regime of the inter-molecular force curve (Figure 5A).

Tapping mode is the next most common mode used in AFM. When operated in air or other gases, the cantilever is oscillated at its resonant frequency (often hundreds of kilohertz) and positioned above the surface so that it only taps the surface for a very small fraction of its oscillation period. This is still contact with the sample in the sense defined earlier, but the very short time over which this contact occurs means that lateral forces are dramatically reduced as the tip scans over the surface. When imaging poorly immobilised or soft samples, tapping mode may be a far better choice than contact mode for imaging (Figure 5B).

Figure 4: A) In contact mode AFM the probe directly follows the topography of the surface as it is scanned. The force of the probe is kept constant while an image is measured. B) In tapping mode, changes in probes vibrations are monitored to establish the force of the probe onto the surface. The feedback unit is used to keep the vibrating amplitude or phase constant.

2.2.4 Experimental method

Observations were made with an AFM Nanoscope IIIa of Digital Instruments (Santa Barbara, CA, USA), Cantilevers with a spring constant of 0.03 N/m and silicon nitride tips were used (MLCT-AUHW, Park Scientific, USA). Tips were previously silanized with octadecyltrichlorsilane (OTS, 95%, Aldrich, USA) to turn hydrophilic tips into hydrophobic ones. AFM Fluid imaging cells was used for this work as described by Menchaca et.al.[5] Schematic representation of the liquid cell AFM is shown in figure 13.

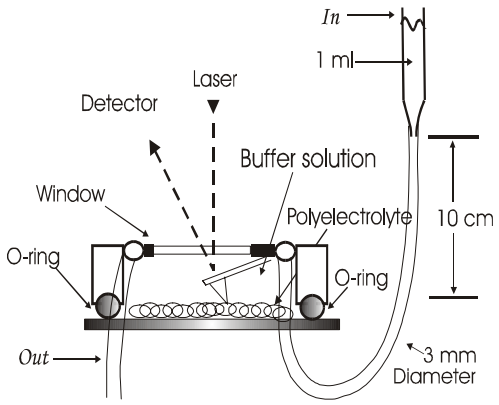

Fig. 5: Schematic representation of the AFM liquid cell set up utilized in this work. Buffer solution was always present during multilayer building. Injection container was 10 cm high. If it was less than 10 cm it does not allow buffer circulation while higher than 10 cm causes buffer draining through the joining of the o-ring.

Height and friction images were captured simultaneously in contact mode, but only the height images are reported. Images were taken at 1 Hz scan rate with a resolution of 512 x 512 pixels. The scanning area sizes were 20, 10 and 5 µm. The glass slides are mounted on AFM piezoelectric. The cell is closed with a silicone o-ring (Digital Instruments, CA, USA). The buffer solution is injected into the cell and an image of the glass surface is taken for testing AFM liquid cell. The positive polyelectrolyte PEI solution is then injected and let for 15 min in contact with the substrate after we were rinsing with 5 ml of buffer solution then the PEI surface is imaged. The negative polyelectrolyte PSS is then injected and let for 15 min, rinsed with 5 ml of buffer solution and the PSS surface is imaged.

2.3 Micro-peeling aspiration technique

Recently one has worked on the short term interaction of the cells and the surfaces of the biomateriales. Several techniques have been proposed to measure the adhesion cell-substratum. One technic is the centrifugation, which uses the centrifuges force to separate cells. The flow camera also has been used, where with flow solution it is tried to separate the cells of the substratum.

Nevertheless these techniques get the force of separation by means of the difference of the separated cells against the cells that remain adhered, which is not a real. The technique of micro aspiration by micro pipette evaluates the cellular adhesion of cell by cell, in addition to that the result are given in nano Pascal's (nP). Statistical analyses give interaction of the cells to the substrate.
The following section covers the basic concepts of the micro-peeling technique used to measure cell adhesion to polyelectrolyte treated surfaces.

2.3.1 Quantification of Cell Adhesion

The micropipets setup is similar to systems previously described in the literature.[6,7] For aspiration of cells, micropipets were pulled to a fine point (model 97, Sutter Instrument Co., Novato, CA) and fractured with a microforge (Alcatel, France) to inner radii of ≈7 µm. The water prefilled pipets were connected to a homemade manometer with pressure transducers (DP103, Validyne Eng.,

Northridge, CA) balanced against atmospheric pressure, as described elsewhere.[8,9] (Figure 6). A micromanipulator (Narishige, Tokyo, Japan) was used to define the micropipet position.

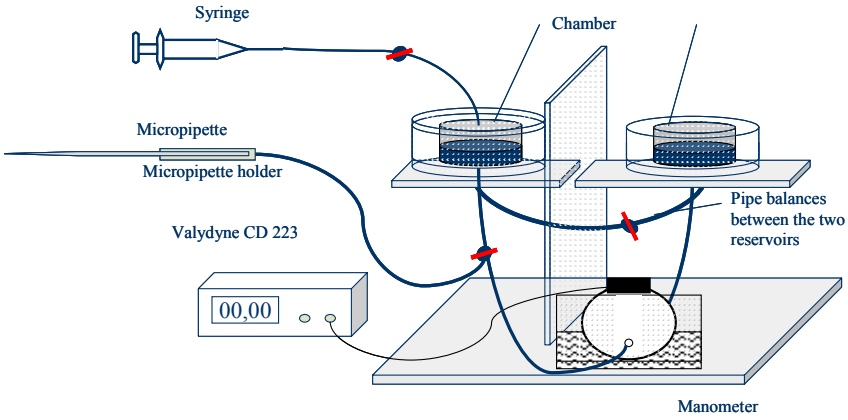

Figure 6 Diagram show the set-up homemade manometer with a pressure transducer (Validyne DP103) with a micromanipulator used in this work.

A homemade Plexiglas holder was designed to maintain the multilayer-coated glass slide vertically. The cell chamber consisted of a section of a polypropylene syringe mounted on a 40 mm diameter cover glass with silicone cement and with a window cut into its side to provide room for pipette micromanipulation[11] (Figure 7).

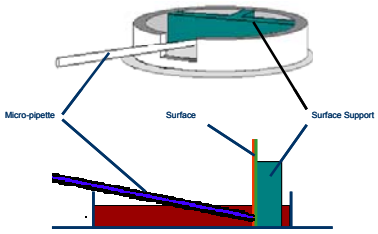

Figure 7: Plexiglas chamber homemade used to manipulate the cells and hold the substrate previously treated with polyelectrolytes.

The chamber is placed on an inverted light microscope (Zeiss Axiovert 10, Germany) equipped with a 32× dry objective, connected to a video camera (SSC-M3, Sony, Japan), S-VHS video recorder (NV-HS-900F, Panasonic, Sony), and monitor (SSM-125CE, Sony, Japan). Recorded images are digitized with a computer equipped with a frame grabber card (LG3; Scion Corp., Frederick, MD) and analyzed with the public domain software NIH Image v.1.6 .

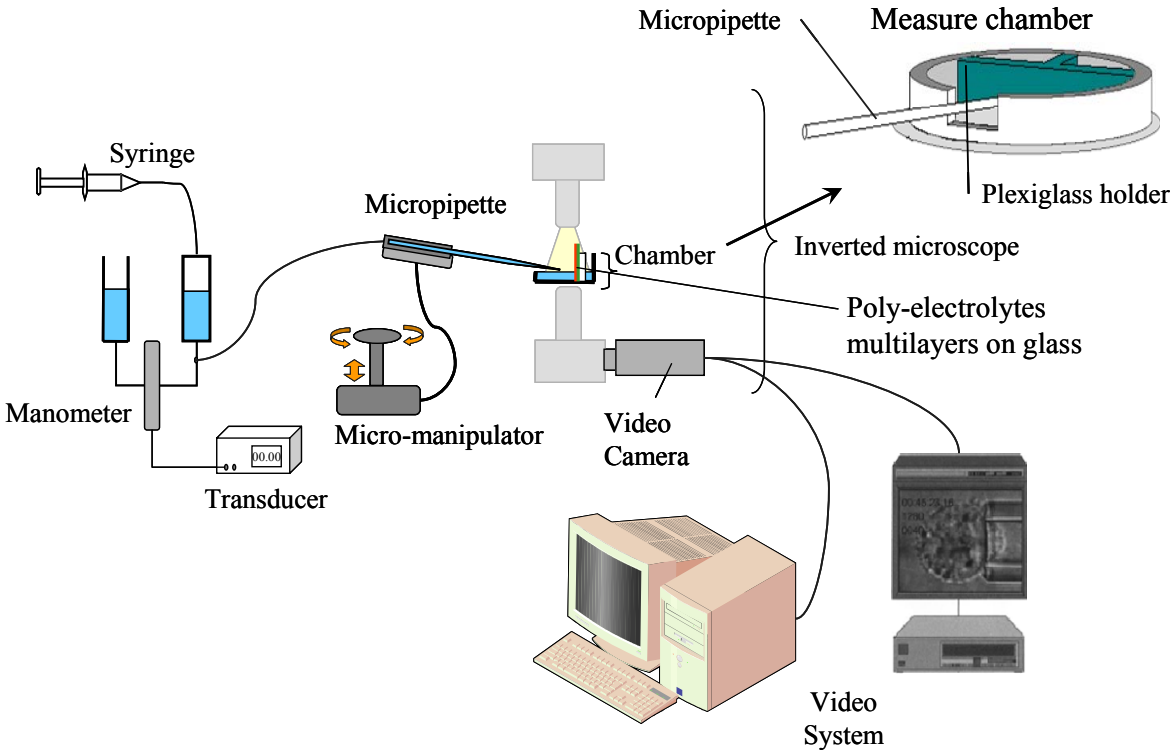

Figure 8: general schema of the set-up used to measure the cell adhesion.

The micromanipulation of the cells in this work was performed on a Nikon TE200 microscope (with camera DXM 1200) equipped with a Marzhäuser motorized stage.

2.3.2 Experimental method

The cells are first deposited at room temperature in the chamber containing either MEM with 10% FCS or only MEM. A single cell is aspirated with a small negative pressure (=50 Pa) within the micropipet and brought horizontally into the vicinity of the polyelectrolyte film.

Then, the negative pressure is removed and the cell is left in this position for 15 seconds to allow it to attach to the film. The micropipette is slowly pulled away from the surface (Figure 9 A and B). After the seeding time (30 min), the micropipette is brought in contact with the cell and a small depression is applied to the cellular membrane. As the speed at which the cell is displaced might influence the measured force, due to the dependence of the rupture force on the retraction rate,[10] the micropipette is pulled away from the surface at a constant speed (≈3 µm/s). If the negative pressure applied to the pipette is not sufficient to create a force that exceeds the cellular adhesion force, the procedure is repeated (Figure 9 C,D,E, and F).

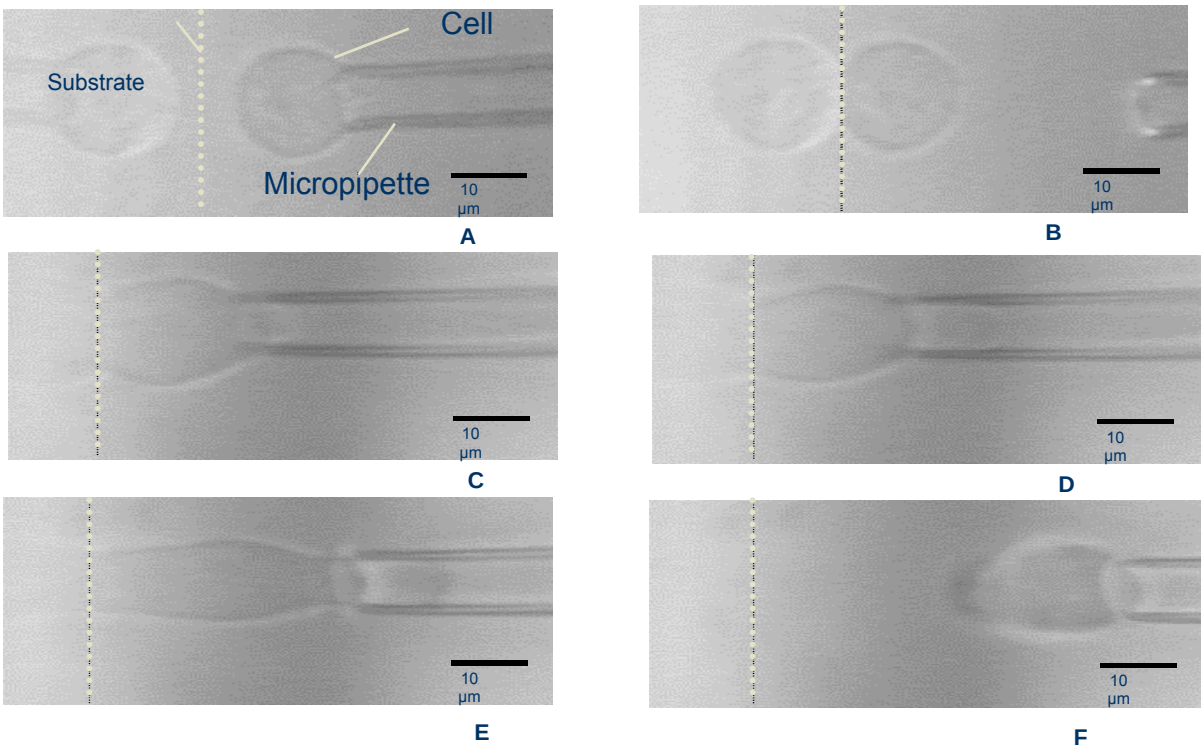

Figure 9: Sequential photographs of one experiment of cell detachment measurement. After the 30 min seeding time, a chondrosarcoma cell was pulled from the multilayer surface with step increases in aspiration depressure (D,E). The pipet holding the cell with a minimum aspiration depressure was moved by micromanipulation until the cell finally detached from the surface (F). (The dotted line represents the cell/film polylelectrolyte film interface.)

The negative pressure is successively increased (by -120 Pa steps) by automatically pulling on an air-filled syringe connected to one of the water reservoirs (Programmable Syringe Pump, Genie-220, World Precision Instruments Ltd, Hertfordshire, U.K.), until the cell adhesion force is exceeded (Figure 9 F). The pipette radius and the depressure applied to the cell membrane are collected in order to calculate the detachment force,[13,11] according to the following formula:

$$F = \pi R_p^2 \Delta P \tag{16}$$

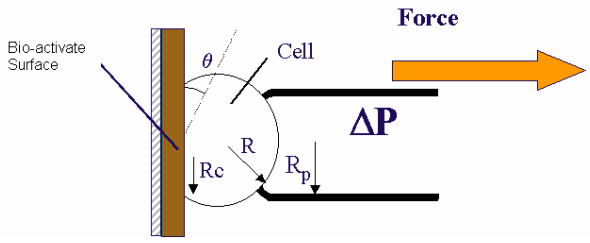

Figure 10: Schematic top view of the experiment: Rp, radius of pipet; ΔP, depressure applied to the cell membrane. A cell approaches a multilayer-coated glass slide which is held by a Plexiglas holder. After 30 min at rest, the cell is progressively detached by step increases in the depression applied to its membrane.

2.4 Transmission electron microscope

The transmission electron microscope (TEM) operates on the same basic principles as the light microscope but uses electrons instead of light. What you can see with a light microscope is limited by the wavelength of light. TEM uses electrons as "light source" and their much lower wavelength makes possible to get resolution thousand times better than a light microscope.

A "light source" at the top of the microscope emits the electrons that travel through vacuum in the column of the microscope. Instead of glass lenses focusing the light in the light microscope, the TEM uses electromagnetic lenses to focus the electrons into a very thin beam. The electron beam then travels through the specimen you want to study. Depending on the density of the material present, some of the electrons are scattered and disappear from the beam. At the bottom of the microscope the unscattered electrons hit a fluorescent screen, which gives rise to a "shadow image" of the specimen with its different parts displayed in varied darkness according to their density. The image can be studied directly by the operator or photographed with a camera.[12]

2.4.1 Experimental methods

TEM was performed using a JEOL JEM-200CX instrument. In order to observe the CdS nanoperticles, TEM samples were prepared by dropping a diluted aqueous solution of CdS nanoparticles onto carbon-coated copper grids.

For TEM observation of the nanocomposite formed by the adsorption of CdS onto polyelectrolyte nanorings, first the carbon-coted grids were put it into the liquid cell AFM system and once structures are obtained confirmed by AFM image, the CdS Nanoparticles were injected and let it in contact by 15 min. The grids were recuperate and put to dry. These grids were first observed in TEM.

2.5 Ultra violet spectroscopy

Different molecules absorb radiations of different wavelengths. An absorption spectrum will show a number of absorption bands corresponding to structural groups within the molecule. For example, the absorption that is observed in the UV region for the carbonyl group in acetone is of the same wavelength as the absorption from the carbonyl group in diethyl ketone.

The absorptions of UV or visible radiation correspond to the excitation of outer electrons. There are three types of electronic transition which can be considered;

1. Transitions involving π, σ, and ν electrons
2. Transitions involving charge-transfer electrons
3. Transitions involving δ and ϕ electrons (not covered in this Unit)

When an atom or molecule absorbs energy, electrons are promoted from their ground state to an excited state. In a molecule, the atoms can rotate and vibrate with respect to each other. These vibrations and rotations also have discrete energy levels, which can be considered as being packed on top of each electronic level.

2.5.1.1 Fluorescence

Absorption of UV radiation by a molecule excites it from a vibrational level in the electronic ground state to one of the many vibrational levels in the electronic excited state. This excited state is usually the first excited *singlet* state. A molecule in a high vibrational level of the excited state will quickly fall to the lowest vibrational level of this state by losing energy to other molecules through collision. The molecule will also partition the excess energy to other possible modes of vibration and rotation. Fluorescence occurs when the molecule returns to the *electronic* ground state, from the excited singlet state, by emission of a photon. If a molecule which absorbs UV radiation does not fluoresce it means that it must have lost its energy some other way. These processes are called radiation less transfer of energy.

2.5.1.2 Intra-molecular redistribution of energy between possible electronic and vibrational states

The molecule returns to the electronic ground state. The excess energy is converted to vibrational energy (internal conversion), and so the molecule is placed in an extremely high vibrational level of the electronic ground state. This excess vibrational energy is lost by collision with other molecules (vibrational relaxation). The conversion of electronic energy to vibrational energy is helped if the molecule is "loose and floppy", because it can reorient itself in ways which aid the internal transfer of energy.

2.5.1.3 Chemiluminescence

Chemiluminescence occurs when a chemical reaction produces an electronically excited species which emits a photon in order to reach the ground state. These sort of reactions can be encountered in biological systems; the effect is then known as bioluminescence. The number of chemical reactions which produce chemiluminescence is small. However, some of the compounds which do react to produce this phenomenon are environmentally significant.

A good example of chemiluminescence is the determination of nitric oxide:

$$NO + O_3 \rightarrow NO_2^* + O_2$$

$$NO_2^* \rightarrow NO_2 + h\nu \quad (\lambda = 600 - 2800 \text{ nm})$$

2.5.2 Experimental method

To deposit CdS nanoparticles onto treated substrates, multilayers were constructed by the LbL self-assembly method. To form the nanorings PEI and PSS polyelectrolytes were employed. Then, the nanoparticles were put it in contact with the polyelectrolyte substrate. After 15 minutes the nanoparticles were washed with 5 ml of MES-TRIS buffer solution (pH 6.8).

The formed nanocomposites were characterized by UV-Vis spectrometry. UV-visible absorption spectra (Perkin Elmer Lambda20 and Ocean Optics 2000); the main absorption band observed at 480 nm in the UV-Vis spectrum pf CdS-stabilized nanoparticles.

2.6 Materials

2.6.1 Polyelectrolytes

All the polyelectrolytes used were prepared in Ultrapure water (Millipore 18.2 MΩcm) at 1 mg/ml concentration. A list of polyelectrolyte used is given in table II.

Table II. Polyelectrolyte used

Polyelectrolyte	Nature	Abbr	pKa	Formula	Mol wt
Poly(L-lysine)	Synthetic degradable	PLL	10.5	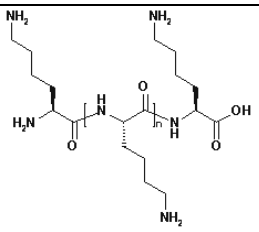	30,000
Poly(L-glutamic acid sodium)	Polypeptide synthetic degradable	PGA	4.3	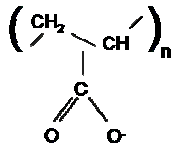	~55, 000
Poly(ethyleneimine)	Synthetic non degradable	PEI	Hard base	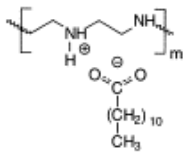	750,000
Poly(4styrenesulfonate sodium)	Synthetic non degradable	PSS	2	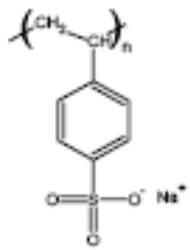	70,000

2.6.2 Polyelectrolyte nanorings formation method

Poly(ethylenimine) (PEI), poly(sodium 4-styrenesulfanate) (PSS) and poly(allylamine hydrochloride) solutions were prepared in water at at 1 mg/ml... TRIS-MES buffers were used for rinsing, which contain 25mM of Tris(hydroximethyl) aminimethane (TRIS) and 2-(N-morpholino)ethanelsulfonic (MES) with 100 mM of NaCl (Sigma, USA), in both cases pH was adjusted with HCl and NaOH solutions at 0.1 M. MES-TRIS buffer was used at pH = 7. All solutions were prepared with degassing ultrapure water (Mill Q-Plus system, Millipore) with resistively of 18.2 MΩcm. The polyelectrolyte solutions were filtered (Millex PVDF, Millipore, USA and PTFE, Nalgene, USA) with filters of 0.10, 0.22 or 0.45µm pore size and the buffer were filtered with filter pore size 0.22.

2.6.3 Nanoparticles synthesis

Nanosized semiconductor has been extensively studied in the last decade, because of the novel optical electronic properties arising from the quantum confinement effect, which vary significantly with the size. Nowadays semiconductor nanoparticles as functional materials have many potential applications, but the disadvantages of nanoparticles liable to aggregate and uncontrollable size hinder the progress.

2.6.3.1 Experimental method

The preparation has been previously described by Zhan (2002).[13] Two types of reverse micelles, denoted as MA and MB, were prepared separately by adding appropriate values, according to the ratio of description as below: W values: 15; Solutions (mL) of CdAc2 or Na2S: 0.740 (concentration 0.033 M); CTAB (g):1.0; Hexanol (mL):1.8;Heptane (mL):11.66. Through ultrasonic or stirring, the turbid solutions of reverse micelle can gradually become into a clear one. Both reverse micelles contained the surfactant CTAB, cosurfactant n-hexanol and oil phase n-heptane. The difference was that MA consisted of CdAc2 (8.45¡Á10-4M) aqueous solution while MB contained Na2S (8.45¡Á10-4M) aqueous solution. Then reverse micelle MB was added dropwise into MA under continuous magnetic (or ultrasonic condition) stirring.

During this process, the CdS nanoparticles were gradually formed. The diameters of the obtained nanowires can be adjusted by varying the W values when preparing the micelles. After the formation of the nanoparticles, the nanoparticles contained reverse micelles were subject to the centrifugation (using the centrifuges with speed at least 6000 r/m). The yellow participates of CdS at the bottom of the centrifuge tube was collected by removing the supernatant liquids. The obtained nanoparticles were then suffered from the extensive washing using ethanol via stirring before the centrifugation. The washing cycle should be repeated at least three times to assure the remove of the surfactant of CTAB. At last the obtained CdS nanoparticles can be dispersed by very short time stirring or ultrasonic in any of solvents as wanted for further assembly with polyelectrolytes into multilayer films.

2.7 Bibilography

[1] Binnig, G., Quate, C.F., and Gerber, Ch. Phys. Rev. Lett. (1986); 56(9), 930.

[2] Gallego-Juárez, J.A. J. Phys. E: Sci. Instrum. (1989); 22, 804.

[3] Meyer, G. and Amer, N.M; Appl. Phys. Lett. (1990); 57(20), 2089.

[4] Putman, C.A.J., De Grooth, B.G., Van Hulst, N.F., and Greve, J; J. App. Phys. (1992); 72(1), 6.

[5] Menchaca J-L, Jachimska B, Cuisinier F and P´erez E 2003 *Colloids Surf.* A 222.

[6] Nugiel, D. J.; Wood, D. J.; Sung, K. L. P. *Tissue Eng.* 1996, *2*, 127.

[7] Sung, K. L.; Yang, L.; Whittemore, D. E.; Shi, Y.; Jin, G.; Hsieh, A. H.; Akeson, W. H.; Sung, L. A. *P. Natl. Acad. Sci. U.S.A.* 1996, *93*, 9182.

[8] Ra, H. J.; Picart, C.; Feng, H.; Sweeney, H. L.; Discher, D. E. *J. Cell Sci.* 1999, *112* (Part 10), 1425.

[9] Discher, D. E.; Mohandas, N.; Evans, E. A. *Science* 1994, *266*, 1032.

[10] Evans, E.; Ritchie, K. *Biophys. J.* 1997, *72*, 1541.

[11] Needham, D. *Methods Enzymol.* 1993, *220*, 111.

[12] Peter Goodhew, Based on Textbook: Transmission Electron Microscopy - Basics by D.B.Williams and C.B.Carter, University of Liverpool

[13] Zhan J., Sun L., Liao C., Yan C. ; Solid State Communications 124 (2002) 45.

Chapter III

3 SAPF Functionalization: Protein Adsorption and Cell Adhesion

Chapter III **54**
3 SAPF Functionalization: Protein Adsorption and Cell Adhesion **54**
3.1 Introduction **55**
3.2 Self Adsorption of Polyelectrolyte Films (SAPF) **55**
3.3 SAPF Protein Functionalization **57**
3.4 Article 1 ..... **58**
3.5 SAPF Protein Functionalized and Cell Adhesion Test **66**
3.6 Article 2 ..... **68**
3.7 Bibliography **69**

3.1 Introduction

Film built by successive adsorption of polycations and polianions, so called, self adsorption polyelectrolyte films (SAPF) developed by Decher is one versatile method of thin film deposition used to modify surfaces. They (SAPF) has been attracted the attention for his significant fundamental and commercial interest with a wide range of applications.

The most important characteristic of polyelectrolyte multilayer is to present always an electrically charged surface. These lead to extensive range of combinations of charge species, which can be used for self-assembled ultrathin films each having different functionalities. This may be the key for design bioactive biomaterials to control biological responses.

In particular, protein adsorption or embedding offers interesting functionalization possibilities. Alternated protein and polyelectrolyte adsorption lead to mixed multi-layered polyelectrolyte/ protein architectures.

Over the last years, the achievements in multilayer assembly functionalization constituted promising approaches with respect to applications in biomaterial coatings, rendering them biocompatible.

The work presented here is aimed to investigate the adsorption of proteins on multilayered polyelectrolyte films deposited on a solid surface at high (0.15M) ionic strength and at different pH values. As well as, the studio of cellular adhesion to multilayer polyelectrolyte film functionalized with RGD.

3.2 Self Adsorption of Polyelectrolyte Films (SAPF)

We consider interesting in the following section the state-of-the-art of alternating adsorption of oppositely charged polyelectrolytes, the so-called “layer-by-layer” method or “sequential adsorption of polyelectrolyte films” (SAPF), for the preparation of thin polymer coatings.

Moreover, the step-by-step procedures allow for a fine structuring in the third dimension. In addition to the preparation of uniform and homogeneous coatings, gratings, gradients or steps of defined height in molecular dimensions can be easily constructed.

The most recent of the self-organization techniques is the alternating adsorption of oppositely charged polyelectrolytes, called layer-by-layer method or "sequential adsorption of polyelectrolyte films (SAPF)[1,2,3]. This particular technique has encountered a strongly increasing interest in the past five years (Fig. 1), due to its striking simplicity.

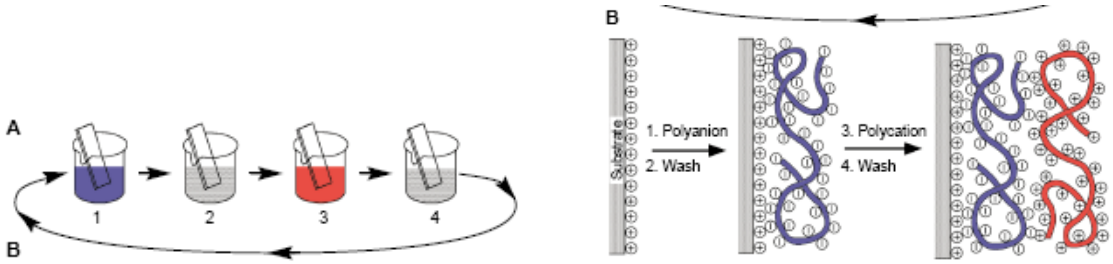

Figure 1: (**A**) Schematic of the film deposition process using slides and beakers. Steps 1 and 3 represent the adsorption of a polyanion and polycation, respectively, and steps 2 and 4 are washing steps. The four steps are the basic build-up sequence for the simplest film architecture, $(A/B)_n$. (**B**) Simplified molecular picture of the first two adsorption steps, depicting film deposition starting with a positively charged substrate. The polyion conformation and layer interpenetration are an idealization of the surface charge reversal with each adsorption step (Decher, 1997).

Many types of charged molecules and nano-objects have been proposed for deposition by the SAPF method, but mostly polyelectrolytes have been employed. Typically, a solid support with a charged surface is exposed to the solution of a polyion of opposite charge for a short time. The practical set-up may be extremely simple, e. g. just dipping the support into beakers filled with the polymer solutions. The dipping can be done manually, although automatic dipping devices may provide some better control[4].

The method is relatively rapid, as adsorption steps last typically between 1 min and 1 h. The amount of adsorbed material is self-limiting. Excess polymer solution adhering to the support is removed by simple washing (Fig. 1). Under proper conditions, charged polymers (polyelectrolytes) are adsorbed, so that the sign of the surface charge is reversed. In consequence, when the substrate is exposed to a second solution containing a polyion of opposite charge, an additional polyion layer is adsorbed. But this reverses the sign of the surface change again. Consecutive cycles with alternating adsorption of polyanions and polycations result in the stepwise growth of polymer films (Fig.1)[5,6,7].

The technique is well suited for automation and has no inherent restriction with respect to form and size of the substrates. Due to multiple electrostatic interactions between the polymers and to the substrate, the films show normally excellent cohesion, as well as adhesion to the substrate. The theoretical understanding of the SAPF technique is open yet, though theoretical approaches are up coming[8]. Kinetically controlled adsorption of polyelectrolytes must lead to overcompensation of the original surface charge, as shown experimentally by recording the f-potential[9,10,11]. Although the SAPF technique is based on electrostatic attraction between positively and negatively charged species, the primary driving force is presumably entropy, not enthalpy.

3.3 SAPF Protein Functionalization

Proteins that embedded retain their activity opens the possibility to construct multilayer incorporating specific ligands, which keep their biological activity and promote the response and adhesion of specific cells. Also, incorporation of proteins that induce biomineralization processes is possible. The controlled incorporation of protein in multilayers however requires first to understand the protein adsorption mechanism as well as, protein structure conformation on these films.

This work is aimed to investigate the adsorption of human serum albumin (HAS) proteins on multilayered polyelectrolyte films deposited on a solid surface at high (0.15M) ionic strength and at different pH values. This experiment were performed in order to know the behavior of HAS at different pH due to this is one of the most important parameter that driving the conformational structure conformation of the film and protein structure and adsorption in the film.

3.4 Article 1

[Signalement bibliographique ajouté par : ULP – SCD – Service des thèses électroniques]

Human Serum Albumin Self-Assembly on Weak Polyelectrolyte Multilayer Films Structurally Modified by pH Changes

Csilla Gergely, Sophie Bahi, Balázs Szalontai, **Hector Flores**, Pierre Schaaf, Jean-Claude Voegel and Frédéric J. G. Cuisinier

Langmuir, 2004, Vol. 20, Pages 5575 -5582

Pages 5575 –5582 :

La publication présentée ici dans la thèse est soumise à des droits détenus par un éditeur commercial.

Pour les utilisateurs ULP, il est possible de consulter cette publication sur le site de l'éditeur : http://pubs.acs.org/cgi-bin/article.cgi/langd5/2004/20/i13/html/la049932x.html

Il est également possible de consulter la thèse sous sa forme papier ou d'en faire une demande via le service de prêt entre bibliothèques (PEB), auprès du Service Commun de Documentation de l'ULP: peb.sciences@scd-ulp.u-strasbg.fr

3.5 SAPF Protein Functionalized and Cell Adhesion Test

Adhesion is the first step in a cascade of events through which cellular interaction with a material surface occurs. Cell surface adhesion molecules play vital roles in numerous cellular processes. Some of these include: cell growth, differentiation, embryogenesis, immune cell transmigration and response, and cancer metastasis. Adhesion molecules are also capable of transmitting information from the extracellular matrix to the cell. There are four major families of cell adhesion molecules. These are the immunoglobulin (Ig) superfamily cell adhesion molecules (CAMs), integrins, cadherins, and selectins[12].

The development of surfaces and polymers functionalized with adhesion ligands has been critical for the elicitation of cell responses in materials for tissue engineering. For example, since the discovery of the functionally significant RGD binding domain of fibronectin for substrate-dependent cell adhesion[13], studies of RGD peptide grafted surfaces have shown that peptide grafting density, ligand localization and the surrounding chemical environment can each affect the cellular processes of many types of cells on functionalized substrates[14,15].

The design of peptide-functionalized surfaces has been extended to micropatterned substrates that localize ligand presentation and control cell shape and function, elucidating the fact that spatial parameters imposed on a cell result in differences in the activation of a cell's physiology through the degree of mechanical constraint on the cell[16,17]. Therefore, the development of novel materials with increasing complexity for cell adhesion and tissue engineering will likely provide new insights into cell physiology as well as provide novel methods of controlling tissue morphogenesis.

In recent years, a novel class of self-assembling materials, composed of self-assembling polyelectrolytes, has emerged as one promising alternative route for the development of dynamic ligand systems. This involves coupling that which is known about the requirements for the control of cell adhesion with the ability to design specific conformations into the molecule governing cell–substrate adhesion behaviour.

In other hand, advances in molecular biology techniques and genetic engineering have provided the means to synthesize precisely determined polypeptide sequences with potential for materials applications[18,19,20].

The following report represents a basic demonstration of the ability to make self-assembling functionalized surfaces through RGD peptide assembly, a necessary first step for the dynamic switching of interfacial interactions using peptide switching.

3.6 Article 2

Physiology and Biochemistry, **111**, 100 (**2003**).

In vitro measurement of the adhesion strength of primary human osteoblasts on modified titanium surfaces.

Arntz Y.[1], Richert L[1], Flores H. [1], Cuisinier F. [1], Frisch B. [2], Picart C[1].
1. INSERM U595-ULP, Faculté de Médecine, 11 rue Humann, 67085 Strasbourg cedex
2. Laboratoire de Chimie Bioorganique, UMR 7514 CNRS-ULP, 74 route du Rhin, 67400 Illkirch, France

Introduction

Titanium is widely used as implant material in dental and orthopedic surgeries for its biocompatibility properties. To improve the incorporation of an implant into the surrounding tissue, mostly osteointegration, a surface treatment must fulfill several biological functions. One promising way of surface modification is based on a new kind of films built by successive adsorption of polycations and polyanions, namely polyelectrolyte multilayers films (PEM) [1] into which active molecules can be incorporated or coupled to the polyelectrolytes. Our work is focused on the measurement of the adhesion of primary cells onto functionalized PEM deposited on titanium samples.

Materials and methods

Films were built with Poly(L-lysine) (PLL) as polycation and Poy(L-glutamic) acid (PGA) as polyanion. For the test of the non-specific cell/film interactions, films containing 6 pairs of layers and terminated either by PLL or PGA were adsorbed on a rough titanium surface : $(PLL\text{-}PGA)_6$ and $(PLL\text{-}PGA)_6$-PLL. The functionalization of the film was achieved by adsorbing the RGD peptide coupled to PLL (PLL-RGD) and a 15AA peptide coupled to PGA (peptide derived from collagen I adhesion site with RGD in central position). $(PLL\text{-}PGA)_6$-PLL-RGD, $(PLL\text{-}PGA)_5$-PLL-PGA-15aa-peptide. These films have been characterized by optical waveguide spectroscopy. Primary human osteoblasts were prepared from a bone explant (dental extraction). Cells were maintained in DMEM medium supplemented with 25 mM HePes, 10 % FCS and antibiotics. Cells were detached from the culture wells and suspended in serum free DMEM. The micromanipulation of the cells was performed on a Nikon TE200 microscope (with camera DXM 1200) equipped with a Marzhäuser motorized stage. Cells were deposited in a chamber and put in contact with the PEM coated sample using a 10µm diameter pipette [2] (Fig 1A). After a 40 min adhesion time, the cells were detached by progressively increasing the negative aspiration pressure into the pipette (Fig 1, B-C).

Fig.1 : Different steps In the experiment. (A) adhesion of a cell, (B) increase in the aspiration pressure, (C) detachment. Scale bar 25 µm.

Results

The adhesion force depends strongly on the PEM outermost layer, either polycation PLL or polyanion PGA. Significant differences were found between the different surfaces, either non-functionalized or functionalized.

Table 1 : Mean adhesion forces on the different types of surfaces.

Surface	Mean adhesion force	Cell number
Rough bare titanium	54 ±3 nN	52
$(PLL\text{-}PGA)_6$	61 ± 4 nN	70
$(PLL\text{-}PGA)_6$-PLL	206 ±12 nN	80
$(PLL\text{-}PGA)_6$-PLL-RGD	115 ±9 nN	40

The lowest adhesion strengths are found on rough bare titanium and on the $(PLL/PGA)_6$ film. High adhesion forces are measured on the PLL ending films and on the films functionalized with PLL-RGD. The mean forces measured with standard error and corresponding cells populations are shown in Table 1. Current measurements concern the 15-mer peptide and a control non adhesive peptide. Full results will be presented at the meeting.

Discussion and conclusion

The short time adhesion of primary osteoblast cells on modified titanium surfaces was measured by the micropipette technique. The modification of the surface was achieved by the deposition of PEM films and their functionalization with adhesion peptides. This new kind of coating represents a very simple and versatile way to functionalize any type of implant surface and to increase the early adhesion of primary cells.

References

1- Decher, G. 1997. Fuzzy nanoassemblies: Toward layered polymeric multicomposites. *Science* 277(5330):1232-1237.
2- Richert, L., Lavalle, Ph., Vautier, D., Senger, B., Schaaf, P. Voegel, J-C., and C. Picart. (2002). Quantification of cell interaction with polyelectrolyte multilayer in the presence and in the absence of serum. *Biomacromolecules*. 3(6):1170-8.

Acknowledgements

The work was supported by the European Community through the SIMI project (Surface Improvements of Metal Implants). H. Flores thanks PROMEP for their PhD scholarships.

3.7 Bibliography

[1] G. Decher, *Science* **277**, 1232–1237 (1997)

[2] G. Decher, M. Eckle, J. Schmitt, B. Struth, *Curr. Opin. Colloid Interface Sci.* **3**, 32–39 (1998)

[3] W. Knoll, *Curr. Opin. Colloid Interface Sci.* **1**, 137–143 (1996)

[4] D. Yoo, S. S. Shiratori, M. F. Rubner, *Macromolecules* **31**, 4309–4318 (1998)

[5] J. F. Joanny*, Eur. Phys. J. B* **9**, 117–122 (1999)

[6] T. Okubo, M. Suda, *J. Colloid Interface Sci.* **213**, 565–571 (1999)

[7] S. Schwarz, K. J. Eichhorn, E. Wischerhoff, A. Laschewsky, *Coll. Surf. A* **159**, 491–501 (1999)

[8] J. F. Joanny*, Eur. Phys. J. B* **9**, 117–122 (1999)

[9] G. B. Sukhorukov, E. Donath, S. Davis, H. Lichtenfeld, F. Caruso, V. I. Popov, H. Mo¨hwald, *Polym. Adv. Technol.* **9**, 759–767 (1998)

[10] F. Caruso, H. Mo¨hwald, *Langmuir* **15**, 8276–8281 (1999)

[11] F. Caruso, M. Schu¨ler, D. G. Kurth, *Chem. Mater.* **11**, 3394–3399 (1999)

[12] Gonzalez-Amaro, R. & F. Sanchez-Madrid (1999) Crit. Rev. Immunol. **19**:389

[13] Ruoslahti E. Annu Rev Cell Dev Biol 1996;12:697–715.

[14] Massia SP, Hubbell JA. JCell Biol1991;114(5):1089–100.

[15] Drumheller PD, Hubbell JA. Anal Biochem 1994;222(2):380–8.

[16] Zhang S, Yan L, Altman M, Lassle M, Nugent H, Frankel F. Biomaterials 1999;20(13):1213–20.

[17] McFarland CD, Thomas CH, DeFilippis C, Steele JG, Healy KE. J Biomed Mater Res 2000;49(2):200–10.

[18] Barron AE, Zuckermann RN. Curr Opin Chem Biol 1999;3(6):681–7.

[19] Holmes TC. Trends Biotechnol 2002;20(1):16–21.

[20] Welsh ER, Tirrell DA. Biomacromolecules 2000;1(1):23–30.

Chapter IV

4 Polyelectrolyte Nanoring Structures

Chapter VI 70
4 Polyelectrolyte Nanoring Structures 70
4.1.1 Introduction 71
4.1.2 Article 3 73
4.1.3 Article 4 82

4.1.1 Introduction

The performance of artificial materials in contact with biological systems is to a large determined by surface interactions. Cell surface interaction is the most critical factor to increase cell adhesion to orthopedic or dental implant. The goal of our research activities is to tailor the surface properties of substrates in such a way, to get favourable interactions.

One way to introduce specific functional groups to a solid surface is to attach polymers to the substrate. The most recent of the self-organization techniques is the alternating adsorption of oppositely charged polyelectrolytes, the so-called "layer-by-layer" method or "sequentially adsorption of polyelectrolyte films" SAPF. A decade ago, Hong and Decher demonstrated the basic principle, i.e. the alternating exposure of a charged substrate to solutions of positive or negative polyelectrolytes, respectively. Provided that each adsorption step leads to charge inversion of the surface, the subsequent deposition finally results in a layered complex, stabilized by strong electrostatic forces. Such SAPF are versatile materials with respect to the incorporation of different compounds or nano-objects and the variety of materials which can be used and furthermore the possibility of combination with other assembly procedures such L-b-L results in a high application potential in a broad range of different areas of materials development.

In order to study "in situ" their surface structure, recently it was introduced a Liquid-Cell AFM technique. In this methodology, external effects are minimized or eliminated during the polyelectrolyte assembling; for instance, drying effects are completely eliminated. An important result of this technique is to show that surface of polyelectrolyte films have a lateral structure; SAPFs form granular domains on their surface which are formed by complex of polyelectrolytes.

In this section, we have report a new polyelectrolyte structures called nanoring which are formed by self assembly of poly(ethylenimine) and poly(sodium 4-styrenesulfonate) (Article III). We present experimental work suggesting that for these polyelectrolyte nanorings, divalent ions are provided by the carbonate ions from air, or directly introduced by cleaning with CO2 or using a carbonate buffer. We determined various parameters influencing nanoring formation. They are mainly related to the preparation method: polyelectrolyte filtration, CO2 presence during the process of formation.

In a second paper presented (Article IV) we show how the filtration of the polyelectrolyte solution with different pore sizes and the carbonate ions concentration play a determinant role that governing

the formation of these structures. Experimentally work show how these two parameters modulate the nanoring formation as consequence of the domain formation of PSS in solution due to their hydrophobic nature, and their interaction with the surface, as well as, screening effect produced by the divalent ions present in the polyelectrolyte solution. This parameter mediated the formation as well as the size of these structures where the competition between electrostatic and hydrophobic interactions plays a critical role. Structural analyses of the images have given complementary information.

4.1.2 Article 3

[Signalement bibliographique ajouté par : ULP – SCD – Service des thèses électroniques]

Self-assembled polyelectrolyte nanorings observed by liquid-cell AFM

J-Luis Menchaca, **Héctor Flores**, Frédéric Cuisinier and Elías Pérez

Journal of Physics.: Condensed Matter*, 2004, Vol.16, S2109-S2117*

Pages 2109 à 2117 :

La publication présentée ici dans la thèse est soumise à des droits détenus par un éditeur commercial.

Pour les utilisateurs ULP, il est possible de consulter cette publication sur le site de l'éditeur : http://www.iop.org/EJ/abstract/0953-8984/16/22/009

Il est également possible de consulter la thèse sous sa forme papier ou d'en faire une demande via le service de prêt entre bibliothèques (PEB), auprès du Service Commun de Documentation de l'ULP: peb.sciences@scd-ulp.u-strasbg.fr

4.1.3. Article 4

[Signalement bibliographique ajouté par : ULP – SCD – Service des thèses électroniques]

Polyelectrolyte Nanoring Structures: Critical Parameters Governing Formation and Structural Analysis

Héctor Flores, J-Luis Menchaca, Ferdinando Tristan, Csilla Gergely, Elías Pérez, and Frédéric J. G. Cuisinier

Macromolecules, 2005, Vol.38, Pages 521 -526

Pages 521 –526 :

La publication présentée ici dans la thèse est soumise à des droits détenus par un éditeur commercial.

Pour les utilisateurs ULP, il est possible de consulter cette publication sur le site de l'éditeur : http://pubs.acs.org/cgi-bin/article.cgi/mamobx/2005/38/i02/html/ma048212u.html

Il est également possible de consulter la thèse sous sa forme papier ou d'en faire une demande via le service de prêt entre bibliothèques (PEB), auprès du Service Commun de Documentation de l'ULP: peb.sciences@scd-ulp.u-strasbg.fr

Chapter V

5 Polyelectrolyte structures as Pattern for Quantum Dots Assembly

Chapter V **88**
5 Polyelectrolyte structures as Pattern for Quantum Dots Assembly **88**
5.1 Introduction **89**
5.2 Polyelectrolyte Nanoring Structures as Nano-patterning for Polyelectrolyte Quantum Dot Assembly **89**
5.2.1 Experimental section: *90*
5.3 Results and discussion **90**
5.4 Conclusions **95**
5.5 Bibliography **96**

5.1 Introduction

Assembly of semiconductor quantum dots (QDs) onto various surfaces is of increasing scientific and technological interest, because it represents a key step for the development of miniaturized, highly functional QD based optoelectronic devices. In order to realize the high functionality of QD based devices, it is critically important to assemble QDs into desired patterns or architectures that meet the device requirements without depressing their electronic and optical properties. To achieve this, there usually needs a patterning structure for QDs assembly.

5.2 Polyelectrolyte Nanoring Structures as Nano-patterning for Polyelectrolyte Quantum Dot Assembly

Self-assembled polyelectrolyte or protein structures on solid substrates have recently emerged as a new kind of patterning structure for QD assembly. It represents significant fundamental and commercial interests with a wide range of applications such as biosensing assemblies as well as biomedical sensors in addition to optoelectronic devices. Actually, chemistry of colloids uses synthetic methods to manipulate the size, structure and properties in order to modify the properties of their surfaces. In optical, electrical and magnetic devices, nanoparticles included will be used in form of thin films.

Generally, semiconductor QDs are used in form of thin films in functional optoelectronic devices. The films can be usually made by spin coating, spraying[1,2], Langmuir-Blodgett film deposition[3,4], or painting nanoparticles matrix mixture[5]. However, the layer-by-layer assembly (LBL) developed by Decher[7] has been proven to be one of the most versatile method of thin film deposition recently used. With this technique, it is possible to assembling QDs in film feature on a polyelectrolyte modified substrate via electrostatic forces, and thus makes it potential for optoelectronic device uses.

The LBL assembly indeed is of special and effective technique to construct polyelectrolyte nanopatternings with a fine control of film architecture and thickness with molecular order and high stability[8]. The deposition process is based on alternating adsorption of oppositely charged polyelectrolytes and bio-macromolecules. Electrostatic force holds the assembly of these ultrathin films together. The LBL assembly lead to extensive range of combinations of charged species, which can be used for self-assembled ultrathin films with different functionalities[9,10]. It has also

been successfully used to construct polyelectrolyte-inorganic nanoparticles composite films for functionalizing the substrate[11,12,13]. This simple and robust technique chemically modifies QD surfaces by controlling the external surface charge and thickness of the deposited layer may allow the integration of coated materials based on external surface chemistry properties, organized over multiple length scales[14].

Here we present polyelectrolyte nanoring structures[15,16] produced by self-assembly process followed by liquid cell AFM technique[17] for patterning CdS quantum dots (QD) assembly.

PEI and PSS were used to form polyelectrolyte nanorings structures. The CdS QD were assembled with polyelectrolyte nanoring patterns onto substrate to create a hybrid film. AFM characterization shows the successful formation of the functionalized hybrid optoelectronic film with dense, uniform and well distributed features. The exceptional possibility as optoelectric devices for the optical hybrid QD based film has been already visualized.

5.2.1 Experimental section:

Nano-patterning of QDs on Polyelectrolyte Nano-ring Structures: Following the obtention of the polyelectrolyte nanoring structures on the glass substrate, one AFM image was taken to observe and analyses the nanostructures, then, 1ml of the CdS QDs solution was added to 5ml of 7.4 pH MES-Tris buffer. This solution was injected directly in the AFM liquid-cell and let in contact during 25 minutes. Following rinsing with 7.4 pH MES-Tris buffer, the AFM image was taken for observation. The construction was continued with monolayers of PEI and PSS.

5.3 Results and discussion

Polyelectrolyte nanoring structure was formed by LBL deposition of PEI and PSS polyelectrolytes in MES-TRIS buffer solution on a glass surface. The structure was obtained with liquid-cell AFM technique, allowing *in-situ* monitoring the polyelectrolyte nanoring formation without drying effects. Figure 1 (left) shows the AFM image of an isolated polyelectrolyte nanoring structure in a 3 dimensional view. With AFM image section analysis as shown in Figure 1 (right), the nanoring structure can be well defined in three parameters: the external diameter (D), the internal diameter (d) and the height (h). This isolated nanoring shown in Figure 1 has an external diameter of ~2.3 μm, internal diameter of ~700nm and a height of ~14 nm. Interestingly, the diameters of the nanorings could be varied from hundreds of nanometers to micron strongly depending on the

preparation parameters; however, their height keeps in range of nanometer dimension from 7-20 nm. This is why we denote them the name of nanoring.

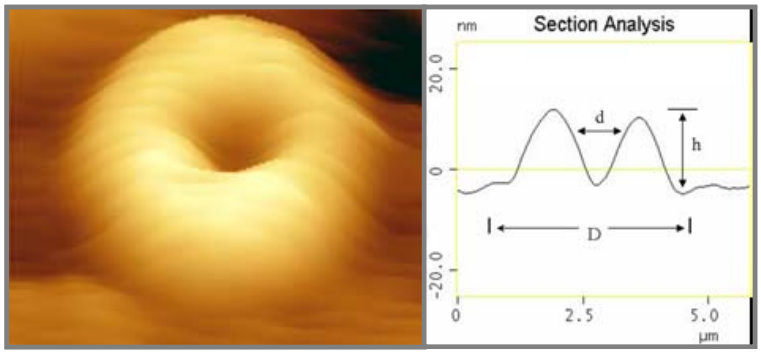

Figure 1. Left: AFM image showing an individual polyelectrolyte nanoring structure with size of ~2.3 µm and height of ~14 nm in a 3 dimensional view; Right: AFM image section analysis defining the polyelectrolyte nanoring structure with three parameters: the external diameter (D), the internal diameter (d) and the height (h). (Image size: 5.2 X 4.2 µm, Z range: 30 nm).

Figure 2 (left) shows low magnification AFM image displaying a number of nanorings formed in a glass substrate. The conditions of formation were controlled in order to obtain this size distribution of nanoring structures. It can be seen clearly that the polyelectrolyte nanorings distribute uniformly on the whole substrate surface. Most of nanorings obtained in this image have the size in several hundreds of nanometers, as a typical section analysis shown in Figure 2 (rigth). The external diameter and internal diameter of one typical nanoring is of 330 nm and 130 nm respectively, [Figure 2 (inset)]. The height of the nanoring is of 7 nm [Figure 2 (inset)].

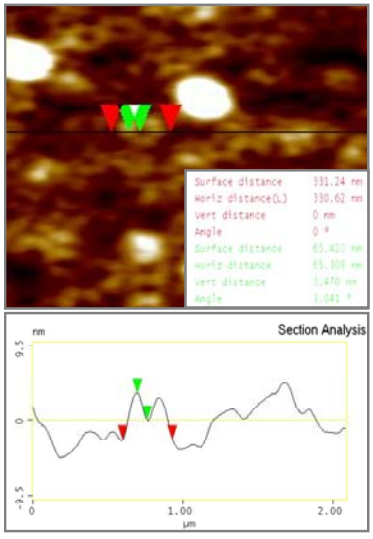

Figure 2. AFM image (top) indicating a number of polyelectrolyte nanorings obtained with PEI-PSS polyelectrolytes in MES-TRIS buffer solution uniformly distributing on a glass surface. Section analysis (bottom and inset) displaying the

sizes of the external diameter (330 nm), internal diameter (130 nm) and height (7 nm) of an individual nanoring. (Image size: 2 × 2 μm, Z range: 5 nm)

By introducing luminescent CdS QDs after the polyelectrolyte nanoring structure formation on the substrate surface, it is able to create a uniform and dense thin film made of highly luminescent CdS QDs with polyelectrolyte coverage. The CdS QDs were made by reverse micelle method previously reported elsewhere[18], possessing a very uniform and monodispersed feature, as TEM image shown in Figure 3 inset (bottom). The QDs have a sharp absorption onset around 450 nm, as shown in Figure 3. According to effective mass equation, the sizes of QDs are evaluated to be around 8 nm, which is consistent with the size observation in TEM image. The QDs have an emission peaking at 575 nm due to the surface state recombination. In order to create the positive charged surfaces, the ratio of Cd^{2+} to S^{2-} was set at 2:1 during the preparation process. This makes QDs possess the positive charge due to the excessive Cd^{2+} adhesion on particle surfaces, thus, possible to be layer by layer assembled onto oppositely charged polyelectrolyte nanoring surfaces based on electrostatic forces.

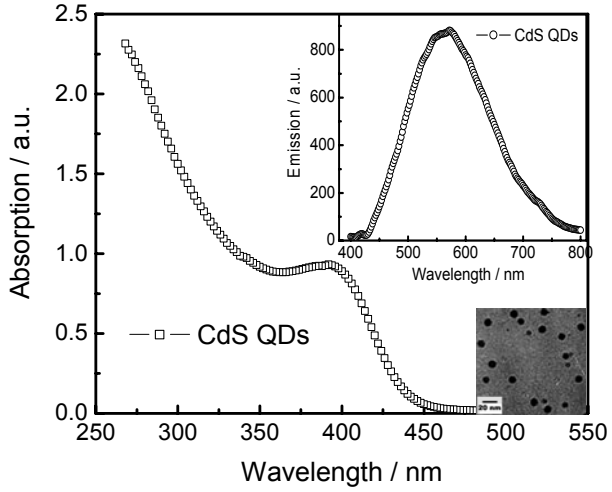

Figure 3. Absorption, emission (inset, top) and TEM image (inset, bottom) of CdS QDs. QD sizes induced from QD absorption onset is around 8 nm, consistent with TEM observation. QDs show a strong emission peaking at 575 nm.

Figure 4 schematically illustrates the self-assembly process of QDs by taking advantage of electrostatic forces between polyelectrolyte nanorings and QDs. First, the polyelctrolyte nanoring structures were created on a glass substrate surface as process 1 described in Figure 4. The polyelectrolyte nanoring surfaces are negative charged due to the top layer assembly of negative charged polyelectrolyte. Then positively charged QDs are absorbed onto the polyelectrolyte nanorings by electrostatic forces as depicted by process 2 in Figure 4. Once the QDs are uniformly deposited on the polyelectrolyte nanoring surfaces, circularly assembly of polyelectrolytes are

followed to cover the QDs (process 3 in Figure 4). Finally the dense hybrid polyelectrolytes/QDs functional films are obtained (process 4 in Figure 4). The QD assembly patterned by polyelectrolyte nanorings followed this protocol.

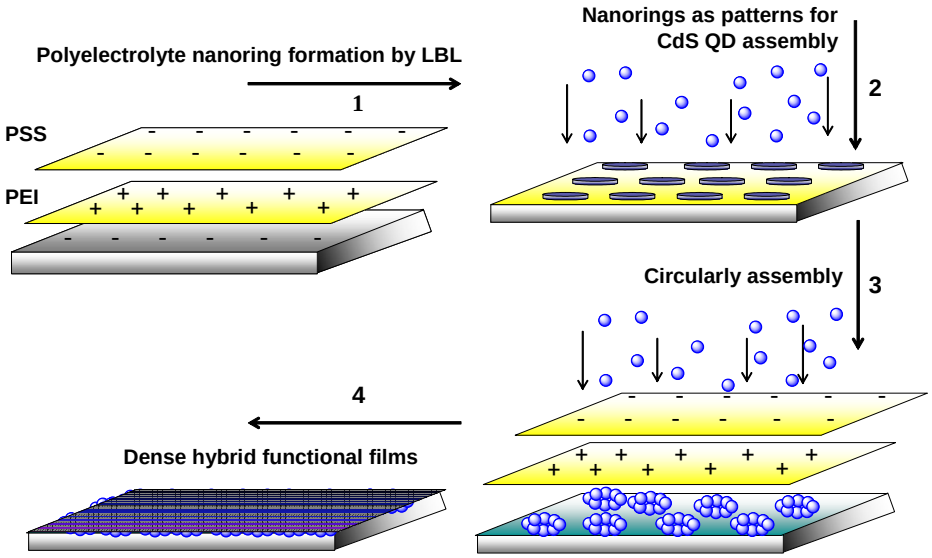

Figure 4. A schematic illustration showing the assembly formation process of hybrid polyelectrolytes/QDs films by using polyelectrolyte nanorings as nanopatterning. Processes 1) PEI and PSS polyelectrolyte layers to form polyelectrolyte nanoring structures, 2) CdS QDs injected on the nanorings substrate, 3) Circularly assembly of polyelectrolytes and 4) Dense hybrid polyelectrolyte/QD optical functional films.

Figure 5 shows the assembly process monitored by AFM. The polyelectrolyte nanorings were first obtained by successive deposition of PEI and PSS buffer solution [(Figure 5 A (top)]. These nanorings have the same dimensional parameters [Figure 5 A (bottom)] as we introduced in Figure 2. Then CdS QDs were injected for electrostatic assembly onto polyelectrolyte nanoring patterns. Figure 5 B (top: height mode) indicates the film feature after CdS QD deposition, showing the formation of a homogonous QDs layer. This can be seen more clearly from the reflection image in Figure 5 B (bottom). Interestingly, some of nanoring patterns of QDs assembles on the polyelectrolyte surface was observed, as shown by the white arrows in Figure 5 B (top). This is substantial evidence that polyelectrolyte nanorings can be used as patterning structure for QDs assembly. The homogonous QD layers can then be covered by continue deposition of polyelectrolytes. Figure 5 C (top: height mode and bottom: reflection mode) displays the further coverage of QD layer with following deposited PEI/PSS polyelectrolytes. Clearly, the complete coverage of QD layer by polyelectrolyte layers was achieved, as evidently shown by the reflection image in Figure 5 C (bottom). It should be noted that the polyelectrolyte/QD construction can be

continued to get desired film thickness, and it is able to add other nanoparticles or objects during the film build-up process.

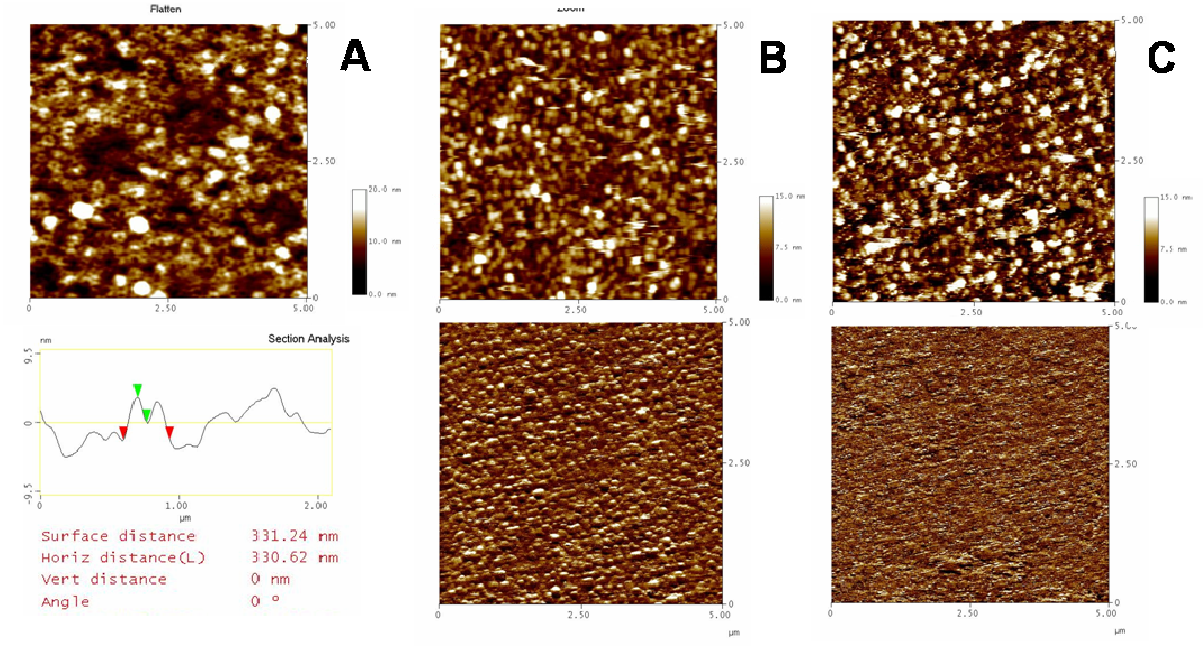

Figure 5. AFM images monitoring the assembly formation process of dense hybrid optical functional polyelectrolytes/QDs films by using polyelectrolyte nanorings as nanopatterning. A) Polyelectrolyte nanoring structures obtained after sequential adsorption of PEI and PSS polyelectrolytes onto glass substrate (top: height mode and bottom: section analysis). B) Polyelectrolyte nanoring structures after CdS QD injection, showing the homogenous QD layer formation. The white arrows in the top image (height mode) show the nanoring-like QD assembles patterned by polyelectrolyte nanorings; while the bottom image (reflection mode) displays more clearly the homogeneousness of QD layer. C) Dense hybrid film obtained after two more layers of PEI-PSS deposition. The images (top in height mode and bottom in reflection mode) show the complete coverage of QD layer by polyelectrolyte layers. (Image size: 5 x 5 µm, Z range: 10 nm).

Fig. 6 show TEM images obtained from carbon-coated grids from the AFM experiments. Left image show some nanorings without CdS nanoparticles. Right image show nanoparticles in non random distribution. For these experiments the used particles were negatively charged. Is possible to observe nanopartcile aggregates ranged in 40 nm in size that appears distributed in the canter of our nanoring structure. This could be related to the electric charge of the structures. If we observe in the AFM experiments the CdS particles were let it positively charged using CTAB. These give us a homogeneous distribution of the particles. We believe that is possible to change the distribution of the particles by using the charge distribution of our nanorings. However, more studies are necessary to clear understand this phenomenon.

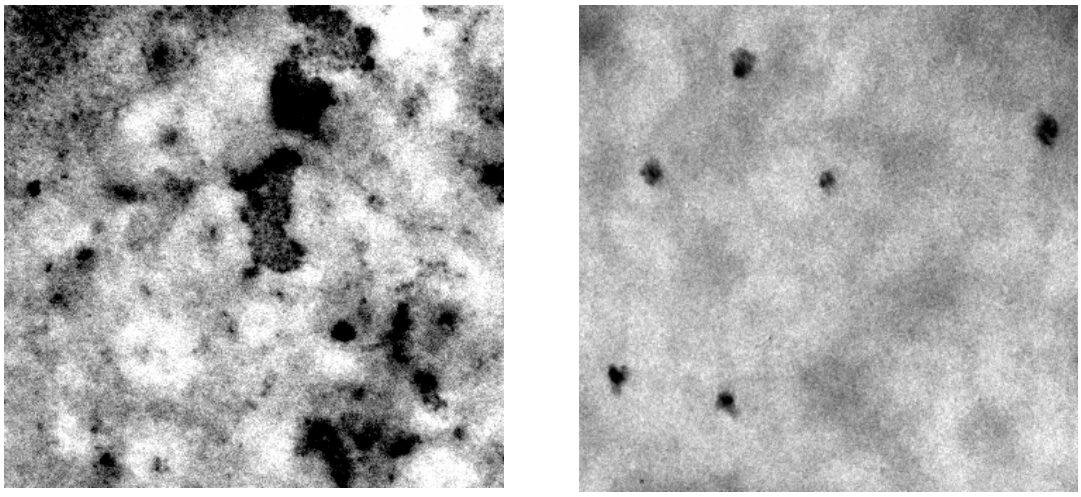

Fig. 6 Tem images of nanorings and nanocomposite made of polyelectrolyte nanorings and CdS nanoparticles. Left, we can observe some nanorings well formed. Right image, we note that the distribution of the nanopartilces aglometartes are not random. WE believe that these agglomerates are attracted to the center of the structures due to the charge distribution of the nanoring.

5.4 Conclusions

In this experimental work, we presented a novel method for CdS QD assembly by using self-assembled polyelectrolyte nanoring structures as nanopatterning. It shows that dense, uniform and QD well distributed functionalized optical film can be obtained via CdS QD assembly onto polyelectrolyte nanorings. The driving force for the film construction is based on the pattering function of polyelectrolyte nanorings with electrostatic force, which enables the uniform dispersion of QD on polyelectrolyte surface, and allows subsequent coverage of QDs with successive polyelectrolyte deposition to enhance the optical stability of QDs and film density. The potential application of these novel structures of polyelectrolytes has great implication for industry and medicine. This assembly method can be adapted to assembly special QD surfaces potential for optical, magnetic or sensor devices. Further theoretical and experimental work is on the way to understand this novel polyelectrolyte pattern system.

5.5 Bibliography

[1] Chauhan P, Annapoorni S, Trikha SK. Bull. Matter. Sci. 1998, 21, 381-385.

[2] Barnes KA, Karim A, Duglas JF, Nakatani AI, Gruell H, Amis EJ. Macromolecules, 2000, 33, 4177-4185.

[3] Salata OV, Dobson PJ, Hull PJ, Hutchison JL. Thin Solid Films, 1994, 251, 1-3.

[4] Phent M, Schultz DL, Curtis CJ, Jones KM, Ginley DS. Appl. Phys. Lett. 1995, 67, 2176-2178.

[5] Cao X, Mello S, Sui G, Mabrouki M, Rastogi V, Chen T, DeFrank JJ, Leblanc RM. Langmuir, 2002, 18, 7616-7622.

[6] O'Hara PC, elbart WM. Langmuir 1998, 14, 3418-3424

[7] Decher G. *Science* **1997**, 277, 1232-1237

[8] Articles INSERML stability of polyelectrolytes

[9] Articulo schilla protein and polyelectrolytes

[10] Joly S. Kane R, razilovski L, Wang T, Wu A, Choen R, Thomas E, Rubner M. Langmuir 2000, 16, 1354-1359.

[11] Ostrander JW, Mamedov AA, Kotov NA. J. Am. Chem. Soc. 2001, 123, 1101-1110.

[12] Pastoriza-Santos I, Koktysh DS, Mamedov AA, Giersig M, Kotov NA, Liz-Marzan LM. Langmuir 2000, 16, 2731-2735.

[13] Constantine CA, Gattas-Asfura KM, Mello SV, Crespo G, Rastogi V, Cheng T-C, DeFrank JJ, Leblanc RM. Langmuir, 2003, 19, 9863-9867.

[14] Mayya KS, Schoeler B, Caruso F. Adv. Funct. Mater. 2003, 13, 183.

[15] J-Luis Menchaca, Flores H, Cuisinier F, Perez E. J. Phys. Condens. Matter. 2004, 16, 2109-2117.

[16] Flores H, Menchaca J-L, Tristan F, Gergely C, Perez E, Cuicinier F. Macromolecules, Submitted, 2004.

[17] Menchaca J-L, Jachimska , Cuisinier F, and Perez . Coll. And Surfaces A : Physicochem. Eng. Aspects, 2003, 222, 5-194.

[18] Zang J, Sun L, Liao Ch, Yan C. Solid State Communications, 2002, 124,45-48.

6 Conclusions and Perspectives

The surface modification by addition of polyelectrolyte is a versatile method to tailor the surface properties of the materials. This method allow the possibility of stabilize and immobilize a great variety of biological as well as non biologics. This possibility could be the key that open large potential applications of polyelectrolytes in the industry and medicine.

One of these perspectives of uses is the protein adsorption in a material surface, which gives us the possibility to regulate the host response. The Human Albumin Serum (HAS) is an important biomolecule which play a central role in the body. Here we show how the behaviour of these proteins is changed by the modification of the pH environment. It is suggested that the higher surface rugosity and the decrease the α-helix content at basic pH values could explain this behaviour. These results give us information necessary to the future design of surface treatments of materials which will be in contact with biologic systems.

Another route to self assembly is the covalent immobilization of peptide as RGD on film. RGD is an essential factor for cellular adhesion. We show that the functionalization of polyelectrolytes with RGD protein increases the cell adhesion to material surface previously treated with our polyelectrolyte. We have used a microppeling system to test the short time interaction between cells and surfaces. This technique used gives us important information about cell adhesion to the pre-treated surfaces. These results can be compared with other and statistically analysed.

Finally, we use the liquid cell AFM technique to study the surface structure of substrates treated with polyelectrolytes. We observed that the polyelectrolytes surface have a kinetic when it is followed in situ. We discover new structures called nanoring. We demonstrated the parameters that are critical for their formation.

We observed also at the time of the deposit of PSS on a layer of PEI, the formation of circular structures. We named these structures of the nanorings. These structures are variable sizes of 300 Nm diameters to 2 μm diameter between the various experiments but by experiment, are of very homogeneous size. Such structures had never been observed. We thus sought to include/understand the mechanisms of controls and formation of these structures. These observations were realizes in AFM by using a liquid cell which prevents the appearance of artefacts due to dehydration. We determined that the two parameters which control the size of the nanoring

are the size of the pores of the filters used for the preparation of the solution of PSS and the time of contact of the solutions with the air. Indeed, divalent ions CO3 -- play a dominating role in the formation of this nanoring. It is about a mechanism of car-assembly of hydrophobic complexes of PSS on the surface of film of PEI. The size being controlled by a balance enters the electrostatic repulsions and hydrophobic attractions and under the dependence of the electrostatic interactions between the PEI and the PSS.

We used these new structures as pattern for nanoparticles deposition (Quantum Dots) to modify the optical properties of the materials. Nanorings can also be used as nanoreactor for hydroxapatite crystal nucleation for implant surfaces.

However, we also believe that more work is necessary to clearly understand the polyelectrolyte-protein-cell interaction in order to design innovatory systems with smart properties.